NATIONAL ADVISORY COMMITTEE FOR AERONAUTICS

TECHNICAL NOTE

No. 1595

ANALYSIS OF FLIGHT-PERFORMANCE MEASUREMENTS ON A TWISTED, PLYWOOD-COVERED HELICOPTER ROTOR IN VARIOUS FLIGHT CONDITIONS

By F. B. Gustafson and Alfred Gessow

Langley Memorial Aeronautical Laboratory
Langley Field, Va.

Washington
June 1948

NATIONAL ADVISORY COMMITTEE FOR AERONAUTICS

TECHNICAL NOTE NO. 1595

ANALYSIS OF FLIGHT-PERFORMANCE MEASUREMENTS ON A TWISTED, PLYWOOD-COVERED HELICOPTER ROTOR IN VARIOUS FLIGHT CONDITIONS

By F. B. Gustafson and Alfred Gessow

SUMMARY

Flight-performance measurements were made of a conventional single-rotor helicopter equipped with a test rotor having plywood-covered blades with -8° twist (designated the "alternate" rotor). Data were obtained in the hovering, vertical autorotative-descent, level-flight, climb, and autorotative-glide conditions. The results of these tests are presented together with a comparison of the results with theoretical results and with results of measurements made on the original production rotor.

Both the hovering and the forward-flight performance of the alternate rotor were found to be within a few percent of the values predicted by theoretical treatments already published by the National Advisory Committee for Aeronautics without any increase in the profile-drag characteristics originally assumed in the theory, provided that blade-section stalling was not present.

The alternate rotor, as compared with the original rotor, showed large improvements in performance in all flight conditions for which a comparison was obtained, that is, hovering, level flight, and autorotative glides. These improvements included an increase of more than 300 pounds (or about 15 percent) in hovering thrust at the same power, a reduction of 20 percent in the minimum value of rotor-shaft power required in level flight, and a decrease of 15 percent in the minimum rate of descent of the helicopter in autorotation. In general, about half of the improvement was considered to be due to improved airfoil-section contour and surface conditions of the alternate rotor blades and most of the other half was considered to be due to the differences in twist and solidity.

Because of the lower solidity of the alternate rotor, tip stalling and the increase in vibration due to tip stalling were actually encountered at a lower forward speed than with the original rotor. On the basis of tuft observations and the pilot's comments on the limiting combinations of forward speed and rotational speed (as set by excessive vibration and loss of control resulting from blade stalling), however, it is concluded that, if the two rotors had been built with the same solidity, the

forward speed for occurrence of blade-tip stalling would have been about 15 miles per hour higher for the alternate rotor than for the original rotor. The data obtained did not permit a reliable estimate of the amount of this 15-mile-per-hour gain which should be ascribed to differences in blade twist or the amount which should be attributed to differences in airfoil section.

Vertical autorotation at rates of descent comparable with those previously obtained with positively twisted autogiro blades was measured with the negatively twisted test rotor. The measured rate of descent was approximately 5 percent higher than the value predicted from the available semiempirical theory.

INTRODUCTION

In references 1, 2, and 3, flight measurements of the performance of a conventional, single-rotor helicopter equipped with its production fabric-covered main-rotor blades are presented. Analysis of the results indicated that agreement with theory (to be discussed in the section entitled "Comparison of Experiment with Theory") could be obtained only by increasing the blade-section profile-drag values used in the theory by about one-third. The need for this increase in profile-drag values was attributed to the relatively rough, deformable surface of the original blades, which was expected to result in larger profile-drag power losses than those predicted by theory, inasmuch as the theory was developed to represent the profile drag of well-built practical-construction sections. Unpublished section data on wind-tunnel test specimens corresponding to the original blades confirmed the need for a roughness factor of this magnitude. Initial flight tests of a plywood-covered rotor (designated the alternate rotor) also suggested that, with blades having smoother and more rigid contour, rotor drag-lift ratios that agreed with the theoretical values (with no change in the original profile-drag assumptions) could be attained.

It appeared desirable, therefore, to extend the tests on the alternate rotor, inasmuch as the data so obtained would be more suitable for comparison with theory than the results of the tests on the original rotor and inasmuch as the magnitude of improvement indicated was sufficient to be of notable practical significance. The data were further expected to provide a good starting point for systematic tests of the effect of rotor parameters such as blade twist. The results of the extended tests of the alternate rotor, which were conducted in consideration of the foregoing factors, are presented herein. The flight conditions included hovering, vertical autorotative descents, level flight, climb, and autorotative glides. These results are correlated with theory, and the performance gains over the original rotor are evaluated. The effects of the built-in twist and the lower solidity of the alternate rotor are estimated for the comparison of the performance of the

two rotors in order to indicate the amount of the gains which is due to improved airfoil characteristics.

SYMBOLS

W	gross weight of helicopter, pounds
b	number of blades per rotor
R	blade radius, feet
r	radial distance to blade element, feet
c	blade-section chord at radius r, feet
c_e	equivalent blade chord, feet $\left(\frac{\int_0^R cr^2\,dr}{\int_0^R r^2\,dr}\right)$
σ	rotor solidity $(bc_e/\pi R)$
θ_m	average main rotor-blade pitch at the 3/4 radius, uncorrected for play in linkage or for blade twist caused by air loads, degrees
ρ	mass density of air, slugs per cubic foot
ρ_o	mass density of air at sea level under standard conditions, 0.002378 slug per cubic foot
V_c	calibrated airspeed (indicated airspeed corrected for instrument installation errors; can be considered equal to $V\sqrt{\rho/\rho_o}$ herein), miles per hour
V	true airspeed of helicopter along flight path, miles per hour
V_h	horizontal component of true airspeed of helicopter, miles per hour
V_v	vertical component of true airspeed of helicopter, feet per minute
Ω	rotor angular velocity, radians per second

γ angle of climb $\left(\tan^{-1}\frac{V_v}{88V_h}\right)$

α rotor angle of attack; angle between projection in plane of symmetry of axis of no feathering and line perpendicular to flight path, positive when axis is pointing rearward, radians (The axis of no feathering is defined as the axis about which there is no first harmonic feathering or cyclic pitch variation.)

μ tip-speed ratio $\left(\frac{V\cos\alpha}{\Omega R}\right)$

$\Delta\alpha_f$ correction to fuselage angle of attack to allow for rotor downwash, degrees (assumed equal to $-57.3C_L/4$)

α_{f_c} corrected fuselage angle of attack, degrees

α_r blade-element angle of attack, measured from line of zero lift, radians

$\alpha_{(1.0)(270^\circ)}$ blade-element angle of attack at tip of retreating blade at 270° azimuth angle, degrees

c_{d_o} section profile-drag coefficient

L rotor lift, pounds

D rotor drag, pounds

T rotor thrust, pounds

Q rotor-shaft torque, pound-feet

$C_{L_{uncor}}$ rotor lift coefficient, uncorrected for air loads on fuselage $\left(\frac{W\cos\gamma}{\frac{1}{2}\rho V^2\pi R^2}\right)$

C_L rotor lift coefficient $\left(\frac{L}{\frac{1}{2}\rho V^2\pi R^2}\right)$

C_D rotor drag coefficient $\left(\frac{D}{\frac{1}{2}\rho V^2\pi R^2}\right)$

C_T rotor thrust coefficient $\left(\frac{T}{\pi R^2 \rho (\Omega R)^2}\right)$

C_Q rotor-shaft torque coefficient $\left(\frac{Q}{\pi R^2 \rho (\Omega R)^2 R}\right)$

M rotor figure of merit $\left(0.707 \frac{C_T^{3/2}}{C_Q}\right)$; the factor 0.707 is included to make the maximum (ideal) figure of merit equal to unity

$\left(\frac{D}{L}\right)_o$ rotor profile drag-lift ratio

$\left(\frac{D}{L}\right)_{o_t}$ rotor profile drag-lift ratio as calculated from theory

$\left(\frac{D}{L}\right)_{o_m}$ rotor profile drag-lift ratio as calculated from measured quantities

$\left(\frac{D}{L}\right)_{p_t}$ parasite-drag contribution of tail rotor divided by main-rotor lift

$\left(\frac{D}{L}\right)_{p_f}$ parasite drag of fuselage, rotor head, and blade shanks, divided by main-rotor lift

$\left(\frac{D}{L}\right)_c$ drag-lift ratio representing angle of climb, positive in climb $\left(\tan^{-1} \frac{V_v}{88 V_h}\right)$

$\left(\frac{D}{L}\right)_i$ rotor induced drag-lift ratio

$\left(\frac{D}{L}\right)_r$ rotor drag-lift ratio; ratio of equivalent drag of rotor to rotor lift $\left(\left(\frac{D}{L}\right)_o + \left(\frac{D}{L}\right)_i\right)$

$\frac{P}{L}$ shaft power parameter, where P is equal to rotor-shaft power divided by velocity along flight path and is therefore also equal to drag force that could be overcome by the shaft power at flight velocity

APPARATUS

The twisted, plywood-covered rotor (designated the "alternate" rotor to distinguish it from the original-production rotor) was flown on a typical helicopter, a general view of which is shown in figure 1. The dimensions and pertinent characteristics of this helicopter are shown in figure 2, and a more detailed description can be found in reference 1. The plan forms of the alternate and original blades are shown in figures 3(a) and 3(b).

The alternate rotor blades had a linear twist of -8° (0.45 deg per ft; tip pitch lower than root pitch) and a relatively low solidity ($\sigma = 0.042$). The blades were plywood covered and were designed with a reflexed NACA 23015 airfoil section; the actual profile differed materially from the true section even after all flats and depressions were faired out with filler. When the blades were received for the tests, they were not aerodynamically smooth, because pitting, grain, flat spots, and other lack of fairness were noted at numerous points. Also, between the leading-edge abrasion strip and the plywood covering there was a U-shaped furrow approximately 1/64 to 1/32 inch in both width and depth. Prior to the initial tests, filler was applied only to the most pronounced discontinuities; the U-shaped furrow was not completely eliminated although the surface was, in general, made smooth. Limited hovering and forward-flight tests were run with the blades in this condition, which is hereinafter designated "before refinishing." After these initial tests, leading-edge templets for representative stations were used to assist in further refinishing and improvement of contour. Although extensive filling and sanding were done in a manner to improve the fit of the templets and although all flat spots were eliminated, it was not feasible to build up the forward part of the rotor blade to a true contour as regards shape and maximum thickness. The blades were considered to be aerodynamically smooth, however, and were wiped clean of grease, bug spatters, and dust before each flight. Some additional hovering data, most of the forward-flight data, and all of the autorotation data were taken with the blades in this smooth condition.

INSTRUMENTATION AND METHODS

The instrumentation and methods employed in measuring rotor performance have been adequately described in references 1 and 3 and need

not be repeated herein. Some special devices which were used to insure zero horizontal airspeeds in the hovering and vertical-flight conditions are, however, worthy of mention.

Both recorded and visual indications of longitudinal deviations from the vertical were obtained in the vertical-descent tests by using a standard NACA yaw-vane indicator and recorder; the transmitter was mounted on a short boom extending from the left landing wheel axle. (See fig. 4.) The attitude of the fuselage during the descent was allowed for in setting the zero position for the NACA yaw vane. Lateral deviations were recorded by a differential-pressure yaw head which was mounted vertically at the end of the airspeed boom (fig. 5) and which was connected to an NACA pressure recorder. A wool tuft on the end of the airspeed boom provided a visual indication of the lateral flow direction as did also the swivelling airspeed heads.

In addition to the equipment employed in vertical descent, forward motion during hovering was avoided with the aid of a pith-ball indicator in the cockpit, which was connected to a double-end pitot head and which responded to forward and backward velocities of approximately 2 or 3 miles per hour. A general view of the cockpit instrumentation, which includes the pith-ball indicator (indicated by an arrow), is shown in figure 6.

REDUCTION OF DATA

The methods of reducing the data obtained in various flight conditions are either apparent by definition or have been explained in references 1 and 3. It is well, however, to review briefly the manner in which the coefficients that are used in presenting the forward-flight and vertical-descent data are calculated.

Rotor drag-lift ratio $\left(\frac{D}{L}\right)_r$ was calculated for the forward-flight condition from the general performance equation expressed in coefficient form as

$$\frac{P}{L} = \left(\frac{D}{L}\right)_r + \left(\frac{D}{L}\right)_{p_f} + \left(\frac{D}{L}\right)_{p_t} + \left(\frac{D}{L}\right)_c$$

For each data point, values of $\frac{P}{L}$, $\left(\frac{D}{L}\right)_{p_f}$, $\left(\frac{D}{L}\right)_{p_t}$, and $\left(\frac{D}{L}\right)_c$ were determined from measured data. The quantity P, which represents the total equivalent helicopter drag, was calculated from recorded shaft-torque values and values of rotor rotational speed, whereas the parasite drag-lift ratio of the fuselage $\left(\frac{D}{L}\right)_{p_f}$ was calculated from full-scale

wind-tunnel tests (reference 4) of the fuselage and airspeed boom of the test helicopter. The parasite-drag coefficients used are given in figure 7 of reference 1. The tail-rotor parasite drag-lift ratios, which are quite small, were obtained by use of the known fixed tail-rotor shaft angle and the measured tail-rotor shaft horsepower by the method of reference 1. Values of $\left(\frac{D}{L}\right)_c$, which represent the tangent of the angle of climb, were determined from the airspeed and the rate of climb; in glides, the quantity $\left(\frac{D}{L}\right)_c$ is negative. The rotor lift L was calculated by multiplying the helicopter gross weight by the cosine of the climb or glide angle and subtracting the fuselage lift. Rotor thrust was assumed equal to the rotor lift in level flight and equal to the rotor lift divided by the cosine of the rotor angle of attack in climbs and glides, at which the rotor angle of attack becomes relatively large.

The measured rotor profile drag-lift ratio $\left(\frac{D}{L}\right)_{o_m}$ was obtained by subtracting an induced drag-lift ratio $\left(\text{assumed equal to } \frac{C_L}{4}\right)$ from $\left(\frac{D}{L}\right)_r$.

The rotor drag coefficient in vertical autorotative descent was obtained from the known gross weight of the helicopter, the measured rate of descent, and the air temperature and pressure by the following formula:

$$C_D = \frac{W}{\frac{1}{2}\rho V^2 \pi R^2}$$

Profile-drag assumptions.- Some studies of the significance of blade-surface condition in relation to the performance of a rotor are given in references 2 and 3. These references also show that accurate section characteristics of practical-construction sections of the rotor are required for precise comparisons between theoretical and measured rotor performance. The theory described in references 5 and 6, which is used for most of the comparisons presented herein, is based on a profile-drag polar which is representative of well-built plywood-covered blades and which has a minimum profile-drag coefficient of 0.0084. Section data are lacking for the alternate rotor but an experimental check of the minimum drag coefficient was obtained by running the rotor at a series of pitch settings near zero degrees with the helicopter on the ground. The results yielded a minimum profile-drag torque coefficient equal to 0.000038, which was computed as the difference between the measured torque coefficient and the small calculated induced value. The equivalent minimum profile-drag coefficient was then calculated as 0.008. Agreement between the theoretical drag polar (involving

three terms) assumed in the forward-flight analysis and the actual drag polar thus appears to exist in the low-angle-of-attack region, and it is reasonable to assume that the agreement will be fair up to the actual stalling angle of attack inasmuch as the theoretical drag polar was based on measured characteristics of similar sections. The stalling angle of attack is likely to be materially less than that shown by wind-tunnel tests of polished, accurately-built NACA 230-series airfoil test specimens.

Hovering.- Theoretical hovering performance was computed with the aid of figure 15 of reference 7 and has already been presented and discussed in reference 2. This particular theoretical treatment (given in reference 7) was selected because of its general availability. Although some empirical adjustment is involved, this treatment essentially represents the commonly used vortex theory with nonuniform inflow and with a profile-drag polar, which for the present tests results in an equivalent drag coefficient of about 0.014. The use of the relatively high profile-drag coefficient of 0.014 may be considered to take the place of the inclusion of tip losses and rotational losses, which are not otherwise included.

Forward flight.- Theoretical performance for level-flight, climb, and glide conditions was computed from reference 6 for the test rotor and included the effect of the -8° twist present but otherwise used the same assumptions and methods described in reference 5 for untwisted blade The charts of reference 5 were used in computing the theoretical performance of the original rotor with untwisted blades.

Vertical power-off descent.- The theory used for calculating rates of descent in the vertical power-off flight condition is semiempirical, being based on the theoretical rotor equations of reference 6 (which utilize the same profile-drag polar on which the forward-flight performance charts are based) and the experimental curves first presented in reference 8. The data of reference 8 were applied in the manner described in reference 9. The experimental curves give the relation between the total flow through the disk of a rotor in vertical descent and the velocity of descent. In the absence of similar experimental curves for twisted blades, the theory for straight blades was applied to the test rotor, the blades of which have -8° twist.

RESULTS AND DISCUSSION

Comparison of Experiment with Theory

Hovering.- Hovering data obtained at altitude with the alternate rotor are tabulated in table I and are compared with theory and with data obtained before the blades were refinished in figure 7. The data obtained before refinishing were first reported in reference 2.

Figure 7 shows that the present data extend the earlier data to higher thrust coefficients and that no difference due to refinishing is discernable. The improvement in contour brought about by the refinishing process presumably was not sufficient to increase materially the extent of the laminar flow. The figure also shows that the alternate rotor produced 83 percent of the thrust that could be obtained with an "ideal" rotor (that is, a rotor producing uniform inflow and having zero profile drag). The agreement of the measured performance with calculated performance is indicated to be within a few percent.

Level flight.- Test data for level-flight, climb, and autorotative-glide conditions are presented in table II, and values of main-rotor drag-lift ratios and other parameters derived from these data are given in table III. The results of the level-flight performance of the alternate rotor are summarized in figure 8, which shows the main-rotor drag-lift ratios both before and after refinishing plotted against the tip-speed ratio μ. The measured data are grouped according to thrust coefficients, and because losses due to stalling were anticipated, all points having a calculated angle of attack at the tip of the retreating blade greater than 12° are indicated by flagged points. Although no blade-section stall-angle data were available for the test rotor, tuft observations on the rotor and also an analysis of rotor profile-drag-loss data as a function of tip angle (reference 10) resulted in the choice of 12° as the stalling angle. The measured rotor performance is compared in figure 8 with a single theoretical curve representative of the average thrust coefficient at which the data were taken. The figure shows agreement within a few percent between the theory and the unstalled points. The discrepancy between the theory, which intentionally omits any allowance for stalling, and the data for the stalled conditions becomes greater as the stalling increases at the higher tip-speed ratios and thrust coefficients.

As was true for the hovering measurements, no difference is discernable (within the scatter shown) between the comparison with theory obtained before refinishing and that obtained after refinishing. (See figs. 8(a) and 8(b).) The data obtained after refinishing are more extensive and show less scatter in the unstalled conditions. From considerations of the improved technique used in obtaining these data they are further considered to be more reliable, particularly as regards the magnitude of the losses due to stalling. For these reasons, the data obtained before refinishing are omitted in the more exacting analysis that follows.

The data obtained after refinishing have previously been analyzed in reference 10 by plotting the ratio of measured values of drag-lift ratios $\left(\frac{D}{L}\right)_{o_m}$ to theoretical values $\left(\frac{D}{L}\right)_{o_t}$ against calculated tip angle, in order to separate more clearly the effects of stalling from the effects

of thrust coefficient and tip-speed ratio anticipated without stalling. This plot is reproduced in figure 9 and indicates excellent agreement with theory below the stalling angle. The airfoil polar assumed in the performance charts appears to predict correctly the profile drag characteristics of the actual airfoil up to the stall under the dynamic conditions encountered in rotor operation.

Figure 9 also indicates that the theory (with no allowance for stalling) underestimates the rotor profile-drag losses for conditions resulting in calculated tip angles of attack above the stall, the discrepancy increasing in approximately a linear manner with the tip angle. A value of 2 is shown for the ratio of measured to theoretical profile drag-lift ratio when the tip angle is approximately 4° above the tip-section stalling value. The results for a calculated tip angle 4° above the angle at which stalling first occurred are significant in that this angle corresponds to the point at which, in the opinion of the pilot, excessive vibration and control difficulties constitute a limit of operation.

Climbs.- The measured climb data and derived parameters are presented in tables II and III. Because of the limited amount of data obtained in this condition and the different thrust coefficients at which they were acquired, it was not feasible to present the results in the form of a rate of climb against velocity plot or its equivalent. Instead, the ratio of experimental $\left(\frac{D}{L}\right)_o$ to that calculated from theory was computed and values of the ratio given in figure 9, in which the agreement between theory and experiment as a function of calculated tip angle of attack is shown.

Figure 9 indicates that, within the experimental scatter, the conclusions to be drawn from the climb data are the same as those for the level-flight runs. Fair agreement is shown between theory and the data taken in the unstalled condition; the theory (with no allowance for stalling) increasingly underestimates the power expended in profile drag as the tip angle exceeds the blade-section stalling angle.

Autorotative glides.- The measured and calculated performances of the alternate rotor in the autorotative-glide condition, in addition to being listed in tables II and III, are shown in figure 10 in terms of the rotor drag-lift ratio and the tip-speed ratio. The data are grouped according to thrust coefficients, and again a single theoretical curve is drawn representing the average thrust coefficient at which the data were taken (0.0049). It can be seen that the theory correctly predicts the performance of the twisted helicopter rotor in autorotation, because the calculated performance serves as a good fairing for the measured data.

Rotor drag coefficients obtained in vertical autorotative descent are compared in figure 11 with the semiempirical theory representing

blades having solidites of 0.10 and 0.04. The vertical scale represents the rotor drag coefficient, which is a measure of the efficiency of the rotor in vertical descent, in that higher values of the coefficients correspond to lower rates of descent. Blade pitch angles are plotted horizontally. The measured coefficients obtained with the alternate rotor show an average deviation from the predicted values of approximately 10 percent or 5 percent in the rate of descent. The vertical scatter shown by the test points does not allow any conclusions to be drawn about the rate of change of C_D with θ_m. Although the gross agreement is fair, a greater amount of experimental data is desirable before more precise conclusions can be drawn as to the accuracy of the predicted performance in this condition.

From the data given in figure 11, a vertical rate of descent of about 2400 feet per minute at sea level was calculated for the test helicopter equipped with the alternate rotor at a gross weight of 2650 pounds. Figure 11 also includes for comparison a value representing vertical-descent data obtained on the Pitcairn PCA-2 autogiro and first reported in reference 11. The figure shows that the measured coefficients for the helicopter equipped with the alternate rotor and for the PCA-2 autogiro differ by less than the experimental error. The agreement is significant in that it indicates that vertical autorotation at rates of descent comparable with those obtained with positively twisted autogiro blades is possible with negatively twisted blades.

Comparison of Original- and Alternate-Rotor Performance

Hovering.- A comparison of the hovering performance of the original rotor, obtained from reference 2, with that of the alternate rotor is presented in figure 12(a). The comparison afforded by the figure, when interpreted in terms of lifting ability, indicates that at normal take-off rotor speed and full throttle (2250 rpm, $C_Q^{2/3} = 0.0043$) the alternate rotor could produce about 330 pounds more thrust than the original rotor. A detailed discussion of the source of this difference is contained in reference 2, which attributes almost one-half of the difference to the lower drag of the smoother and more rigid surfaces of the alternate rotor. Most of the other half of the difference was ascribed to the higher blade loadings obtained with the lower solidity of the alternate rotor.

Figure 12(b) shows the same results plotted as rotor figure of merit against C_T/σ. The maximum figure of merit reached in the tests is seen to be 0.66 for the original rotor and 0.76 for the alternate rotor. Although plotting against C_T/σ provides a comparison at equal mean lift coefficients, it does not altogether eliminate the primary and readily predictable effects of solidity. The reason for this conclusion is that the lower-solidity rotor must operate at a higher tip speed to provide the same thrust at the same value of C_T/σ. This increased tip speed acts

to increase the profile-drag power losses. By use of the treatment of reference 7, the value of figure of merit of 0.76 obtained for the alternate rotor would appear to be increased to about 0.79 if its solidity were increased to that of the original rotor.

Level flight.- A comparison of the performance of the original and alternate rotors in the level-flight condition is presented in non-dimensional form in figure 13(a). The performance of each of the rotors is shown at an average $C_T = 0.0046$ and was obtained by fairing the measured data having approximately the same C_T. The measured data for the original rotor were taken from reference 1. Conditions involving stalling on the outer part of the retreating blades are indicated by dashed lines in the figure. The performance of both rotors is shown in the familiar form of shaft power plotted against speed in figure 13(b). The curves were obtained from faired curves of P/L plotted against $\frac{1}{\sqrt{C_L}}$ and represent sea-level performance at an average gross weight of 2565 pounds.

Figure 13(b) shows that the alternate rotor required 80 horsepower at a speed of 40 miles per hour, which is the speed for minimum power. This power value represents a 20-horsepower (or 20-percent) saving from the power required by the original rotor at the same speed. Theoretical considerations indicate that a saving of approximately 5 to 10 horsepower may be attributed to the blade twist and the lower solidity of the alternate rotor, whereas its smoother and more rigid surface is considered to account for most of the remaining 15 to 10 horsepower. In the high-speed condition, the difference in power required by the two rotors is reduced to approximately 10 horsepower. The smaller power difference at high speed is attributed to earlier blade stalling on the alternate rotor, as indicated by the dashed lines.

Level-flight stalling limitations.- The earlier blade stalling just mentioned may seem paradoxical at first glance since the difference in both twist and airfoil section would be expected to delay the stalling for the alternate rotor. The lower solidity, however, by increasing the mean blade-section angle of attack, tends to produce earlier stalling. In order to separate these effects as far as possible and to give the results greater generality, the comparison was studied by use of the calculated angle of attack of the retreating tip as a stalling criterion. The tip-angle-of-attack computations of reference 5 for untwisted blades together with corresponding computations (based on reference 6) for twisted blades were used for this purpose. Both tuft observations (reference 10) and the pilot's comments on limiting conditions of operation (as set by excessive vibration and loss of control) showed that the same tip-angle-of-attack criterions were applicable for the alternate rotor as were reported for the original rotor in reference 12, that is, 12° for initial stalling and 16° for the limiting conditions.

Inasmuch as the theory used credits the -8° twist with reducing the tip angle of attack at any given combination of μ and C_T/σ by about

$2\frac{1}{2}^{\circ}$, more extreme combinations of μ and C_T/σ are actually possible without stall for the twisted rotor if the same tip-angle-of-attack criterion is found to apply to both the twisted and untwisted rotors. If the solidity of the alternate (twisted) rotor is assumed to be raised to equal that of the original rotor ($\sigma = 0.06$), then, in order to get the same calculated tip angle of attack at the same C_T/σ, μ must be increased by about 0.05. This increase in μ corresponds to an increase in speed of about 15 miles per hour.

Examination of the problem thus indicates that if the two rotors had been built with the same solidity the effects of stalling would have occurred at a speed about 15 miles per hour higher for the alternate rotor than for the original rotor instead of occurring earlier as was actually the case.

The theory used assumes the inflow velocity to be uniform over the rotor disk both with and without twist, and hence the velocity is unchanged by twist; whereas some appreciable readjustment must be expected to take place at the relatively low speeds covered in the present tests. Further, the use of the tip angle as an index does not allow for the difference in shape of the stalled regions, which might become a significant factor by the time the operating limitation is reached. A part of the 15-mile-per-hour gain just discussed, therefore, may quite possibly have been due to a higher section stalling angle in spite of the identical values of calculated tip angle. The data obtained are not adequate for analysis of this point.

Autorotative glides.— Because of the limited amount of autorotation data obtained with each rotor, it was not feasible to compare the performance of each by fairing the measured data. It has been shown in reference 3 for the original rotor and herein for the alternate rotor that theory adequately predicts the behavior of each rotor in autorotative glides. The theoretical performances of the original and alternate rotors are therefore compared in figure 14 at an average value of $C_T = 0.0049$. The performance of the original rotor was computed (reference 3) with a 28-percent increase in the section-profile drag-lift ratios to allow for the poor surface condition of the original rotor.

At the tip-speed ratio for the minimum rate of descent figure 14 shows a difference equal to 0.045 in drag-lift ratio between the two rotors. This difference corresponds to 160 feet per minute or approximately a 15-percent decrease from the 1080 feet per minute measured with the original rotor, when the helicopter was gliding at approximately 40 miles per hour at standard sea-level conditions and at a gross weight of 2565 pounds. Theory (references 5 and 6) indicates that approximately one-half the decrease in rate of descent is due to the beneficial effects of the twist and solidity of the alternate rotor (the lower solidity results in improved efficiency in this case when operating at fixed rotor tip speed) and that most of the remaining gains are due to improved surface condition.

CONCLUSIONS

Flight-performance measurements were made with the test helicopter equipped with a twisted, plywood-covered rotor (designated the "alternate" rotor). A comparison of the results of these tests with theoretical results already published by the National Advisory Committee for Aeronautics and with results of measurements made with an untwisted fabric-covered rotor (designated the "original" rotor) indicates the following conclusions:

1. Both the hovering and the forward-flight performances of the alternate rotor were within a few percent of the values predicted by existing theory without any increase in the profile-drag characteristics originally assumed in the theory, provided that blade-section stalling was not present.

2. The alternate rotor, as compared with the original rotor, showed large improvements in performance in all flight conditions for which a comparison was obtained, that is, hovering, level flight, and autorotative glides. These improvements included an increase of more than 300 pounds (or about 15 percent) in hovering thrust at the same power, a reduction of 20 percent in the minimum value of rotor-shaft power required in level flight, and a decrease of 15 percent in the minimum rate of descent of the helicopter in autorotation. In general, about half of the improvement was considered to be due to improved airfoil-section contour and surface condition of the alternate rotor blades and most of the other half was considered to be due to the differences in twist and solidity.

3. Because of the lower solidity of the alternate rotor, tip stalling and the increase in vibration due to tip stalling were actually encountered at a lower forward speed than with the original rotor. On the basis of tuft observations and the pilot's comments on the limiting combinations of forward speed and rotational speed (as set by excessive vibration and loss of control resulting from blade stalling), however, it is concluded that if the two rotors had been built with the same solidity the forward speed for occurrence of blade-tip stalling would have been about 15 miles per hour higher for the alternate rotor than for the original rotor. The data obtained did not permit a reliable estimate as to the amount of this 15-mile-per-hour gain which should be ascribed to differences in blade twist or the amount which should be attributed to differences in airfoil section.

4. Vertical autorotation at rates of descent comparable with those previously obtained with positively twisted autogiro blades was measured with negatively twisted blades. The measured rate of descent obtained

with the negatively twisted test rotor was approximately 5 percent higher than the value predicted from the available semiempirical theory.

Langley Memorial Aeronautical Laboratory
National Advisory Committee for Aeronautics
Langley Field, Va. December 19, 1947

REFERENCES

1. Gustafson, F. B.: Flight Tests of the Sikorsky HNS-1 (Army YR-4B) Helicopter. I - Experimental Data on Level-Flight Performance with Original Rotor Blades. NACA MR No. L5C10, 1945.

2. Gustafson, F. B., and Gessow, Alfred: Flight Tests of the Sikorsky HNS-1 (Army YR-4B) Helicopter. II - Hovering and Vertical-Flight Performance with the Original and an Alternate Set of Main-Rotor Blades, Including a Comparison with Hovering Performance Theory. NACA MR No. L5D09a, 1945.

3. Gessow, Alfred, and Myers, Garry C., Jr.: Flight Tests of a Helicopter in Autorotation, Including a Comparison with Theory. NACA TN No. 1267, 1947.

4. Dingeldein, Richard C., and Schaefer, Raymond F.: Full-Scale Investigation of the Aerodynamic Characteristics of a Typical Single-Rotor Helicopter in Forward Flight. NACA TN No. 1289, 1947.

5. Bailey, F. J., Jr., and Gustafson, F. B.: Charts for Estimation of the Characteristics of a Helicopter Rotor in Forward Flight. I - Profile Drag-Lift Ratio for Untwisted Rectangular Blades. NACA ACR No. L4H07, 1944.

6. Bailey, F. J., Jr.: A Simplified Theoretical Method of Determining the Characteristics of a Lifting Rotor in Forward Flight. NACA Rep. No. 716, 1941.

7. Knight, Montgomery, and Hefner, Ralph A.: Static Thrust Analysis of the Lifting Airscrew. NACA TN No. 626, 1937.

8. Lock, C. N. H., Bateman, H., and Townend, H. C. H.: An Extension of the Vortex Theory of Airscrews with Applications to Airscrews of Small Pitch, Including Experimental Results. R. & M. No. 1014, British A.R.C., 1926.

9. Wheatley, John B.: An Aerodynamic Analysis of the Autogiro Rotor with a Comparison between Calculated and Experimental Results. NACA Rep. No. 487, 1934.

10. Gustafson, F. B., and Gessow, Alfred: Effect of Blade Stalling on the Efficiency of a Helicopter Rotor as Measured in Flight. NACA TN No. 1250, 1947.

11. Wheatley, John B.: Lift and Drag Characteristics and Gliding Performance of an Autogiro as Determined in Flight. NACA Rep. No. 434, 1932.

12. Gustafson, F. B., and Myers, G. C., Jr.: Stalling of Helicopter Blades. NACA TN No. 1083, 1946.

TABLE I

SUMMARY OF DATA OBTAINED IN HOVERING ABOVE THE REGION OF GROUND EFFECT WITH ALTERNATE ROTOR

Run	Gross weight, W (lb)	Average atmospheric pressure (in. Hg)	$\frac{\rho}{\rho_o}$	Rotor speed (rpm)	Engine speed (rpm)	Free-air temperature (°F)	Manifold pressure (in. Hg)	Brake horsepower (power charts)	Main rotor power (hp)	Pitch angle (deg)		C_T	C_Q	$C_Q^{2/3}$	M
										Main rotor	Tail rotor				
1	2609	27.93	0.990	215	2004	28	27.12	168	139	11.5	8.2	0.0054	0.000368	0.00514	0.757
2	2652	29.01	1.005	225	2100	40	28.00	174	144	10.7	6.3	.0049	.000327	.00475	.740
3	2650	29.04	1.006	225	2104	40	28.08	174	144	10.7	8.2	.0049	.000325	.00473	.738
4	2644	29.08	1.008	223	2076	40	28.08	174	143	10.7	9.2	.0050	.000332	.00480	.741
5	2632	29.06	1.007	240	2240	40	27.28	179	145	9.4	7.7	.0043	.000271	.00418	.725
6	2629	29.07	1.007	240	2240	40	27.28	179	148	9.4	7.5	.0043	.000276	.00424	.711
7	2612	29.10	1.009	215	2006	40	28.22	171	139	11.5	9.2	.0053	.000360	.00506	.747

NACA

TABLE II

SUMMARY OF DATA OBTAINED IN THE LEVEL-FLIGHT, CLIMB, AND AUTOROTATIVE-GLIDE CONDITIONS WITH ALTERNATE ROTOR

Test run	Calibrated airspeed, V_c (mph)	Average density ratio ρ/ρ_o	True air-speed, V (mph)	Gross weight, W (lb)	Rotor speed (rpm)	Engine speed (rpm)	Rate of descent, V_V (fpm)	Average atmospheric pressure (in. Hg)	Free-air temperature (°F)	Intake air temperature (°F)	Manifold pressure (in. Hg)	Brake horsepower (power charts)	Main rotor power (hp)	Pitch angle (deg)		Shaft inclination (deg)	Center-of-gravity position, ahead of shaft (in.)	Stick position forward (in.) (a)	Stick position left (in.) (a)	Yaw angle (deg)
														Main rotor	Tail rotor					
1	46.2	1.061	44.8	2588	225	2100	0	29.70	35	41	16.93	104	79	-----	-----	-3.1	1.6	3.5	3.2	1.7
2	46.2	1.061	45.4	2582	225	2100	0	29.70	35	41	16.93	104	80	-----	-----	-3.6	1.7	3.6	3.1	1.1
3	48.3	1.062	46.6	2579	241	2250	0	29.71	35	43	16.74	107	82	-----	-----	-3.3	1.7	3.1	2.6	.9
4	48.3	1.061	46.0	2576	241	2250	0	29.70	35	43	16.74	107	82	-----	-----	-3.1	1.7	3.1	2.5	1.8
5	48.3	1.064	45.7	2570	216	2020	0	29.77	35	43	16.81	100	77	-----	-----	-3.3	1.8	4.1	3.5	1.7
6	46.8	1.065	44.7	2564	216	2020	0	29.81	35	43	16.93	101	78	-----	-----	-3.1	1.8	4.1	3.5	1.8
7	56.0	1.060	54.4	2560	225	2100	0	29.67	35	43	18.05	111	88	-----	-----	-5.0	1.9	4.2	3.4	-----
8	55.4	1.059	53.8	2552	225	2100	0	29.65	35	43	17.80	109	89	-----	-----	-5.0	2.0	4.1	3.1	-----
9	56.9	1.059	55.2	2548	242	2260	0	29.63	35	42	17.80	115	93	-----	-----	-5.0	2.0	3.4	2.6	-----
10	56.9	1.054	55.3	2540	242	2260	0	29.50	35	42	17.76	115	91	-----	-----	-5.2	2.1	3.4	2.6	-----
11	54.5	1.015	54.0	2609	216	2020	0	27.82	15	31	17.46	105	91	-----	-----	-4.1	1.4	5.3	4.1	-----
12	54.5	1.020	54.0	2603	215	2010	0	27.97	15	31	17.93	107	89	-----	-----	-4.1	1.4	5.3	4.4	-----
13	39.0	1.019	38.6	2597	226	2110	0	28.00	16	35	16.45	102	81	-----	-----	-2.2	1.5	3.4	3.2	-----
14	38.5	1.022	38.1	2591	226	2110	0	28.07	16	35	16.51	102	80	-----	-----	-2.3	1.6	3.3	3.2	-----
15	38.3	1.012	38.0	2584	241	2250	0	27.75	15	30	16.71	108	87	-----	-----	-2.3	1.6	2.7	3.0	-----
16	38.7	1.016	38.4	2576	241	2250	0	27.86	15	30	16.71	108	87	-----	-----	-2.3	1.7	2.8	2.6	-----
17	37.0	.996	37.1	2572	216	2020	0	27.20	13	30	17.14	103	83	-----	-----	-2.1	1.8	3.6	3.9	-----
18	38.5	.999	38.5	2565	215	2010	0	27.26	13	30	16.71	102	80	-----	-----	-2.3	1.8	3.5	3.7	-----
19	64.9	.964	64.9	2660	226	2110	0	27.55	35	53	21.35	138	113	10.9	1.9	-4.6	1.5	4.9	3.1	1.1
20	65.1	.973	65.1	2648	221	2060	0	27.79	35	49	23.00	146	123	11.9	2.0	-4.8	1.6	5.1	4.0	2.1
21	67.2	.965	67.2	2639	241	2250	0	27.57	35	54	20.41	132	114	9.2	1.2	-5.1	1.7	3.8	2.3	1.8
22	74.5	.967	74.5	2624	240	2240	0	27.63	35	50	23.69	153	135	10.4	1.0	-7.2	1.9	4.2	2.7	.6
23	79.1	.969	79.1	2609	239	2230	0	27.68	35	50	25.91	173	152	11.2	1.1	-8.4	2.0	4.1	3.1	2.1
24	74.2	.972	74.2	2594	226	2110	0	27.73	35	47	26.10	167	148	12.4	1.6	-7.4	2.2	4.8	4.1	3.0
25	38.1	.936	39.4	2648	240	2240	0	27.56	50	62	28.90	184	83	8.0	1.6	-0.9	1.6	2.3	2.0	2.1
26	42.5	.938	43.9	2624	225	2100	0	27.56	50	68	29.60	184	83	9.4	1.5	-1.8	1.9	2.9	2.4	1.2
27	69.6	.964	70.9	2599	225	2100	0	28.58	55	68	26.25	162	144	12.4	2.0	-6.4	1.5	--------	--------	.9
28	45.1	.964	45.9	2587	214	2000	0	28.62	38	77	17.62	102	81	10.0	1.4	-1.8	1.6	--------	--------	-.2
29	42.5	.874	45.4	2569	216	2020	0	25.57	48	63	19.13	112	95	11.4	3.1	-1.4	1.8	--------	--------	-2.0
30	82.2	1.000	82.2	2554	244	2280	0	30.01	60	72	28.85	191	169	10.9	1.4	-9.4	2.0	--------	--------	.4
31	80.0	.952	82.0	2496	245	2290	0	29.86	80	98	28.72	187	161	11.0	1.1	-9.4	1.5	--------	--------	.7
32	78.4	.950	80.4	2493	245	2290	0	29.86	82	96	28.35	183	151	10.6	1.2	-8.9	1.6	--------	--------	.6
33	79.2	.961	80.8	2478	245	2290	0	29.86	76	88	28.80	188	158	10.9	1.1	-9.2	1.7	--------	--------	-----
34	32.3	1.010	32.1	2612	225	2100	753	28.34	26	35	27.26	173	150	10.8	4.3	-1.7	1.4	3.3	4.4	.5
35	34.1	1.018	33.8	2610	225	2100	790	28.36	23	30	27.23	174	151	-----	-----	-1.9	1.4	3.2	4.4	1.3
36	45.2	1.038	46.2	2612	224	2090	807	28.58	17	30	27.44	173	154	-----	-----	-3.4	1.4	4.2	4.7	-----
37	33.0	1.004	32.8	2642	240	2240	771	29.10	30	37	26.23	183	153	9.6	3.6	-1.4	1.5	1.9	2.3	2.1
38	28.0	1.005	27.9	2665	225	2100	607	28.23	45	42	27.15	170	144	10.7	5.3	-1.3	1.2	2.1	2.8	-1.9
39	45.5	.925	47.3	2666	217	2030	304	27.09	50	62	26.25	162	134	12.9	2.9	-1.7	1.4	4.6	4.7	2.6
40	49.8	.934	51.0	2630	220	2050	509	27.75	50	62	26.89	175	140	12.4	3.2	-2.7	1.8	3.9	3.8	.4
41	63.1	1.034	62.0	2608	227	2120	-1238	28.81	23	-----	-----	-----	-5.6	-----	-----	-4.6	1.4	4.8	1.5	-.1
42	52.5	1.040	51.0	2599	224	2090	-1053	28.62	17	-----	-----	-----	-5.6	-----	-----	-2.2	.5	3.5	1.6	-----
43	53.1	.944	54.6	2642	223	2080	-1065	27.70	30	-----	-----	-----	-5.5	4.8	-1.0	-2.3	1.7	3.0	1.1	-1.0
44	49.2	.958	50.3	2618	218	2040	-1100	28.29	30	-----	-----	-----	-5.4	5.6	-.8	-2.0	1.9	3.0	1.2	3.4
45	43.0	.933	44.7	2563	220	2050	-1022	27.66	32	-----	-----	-----	-4.5	5.6	1.1	-1.3	1.9	-----	-----	2.0

[a] Cyclic pitch variation in degrees from mean value is 1.25 × stick position.

TABLE III

MAIN ROTOR DRAG-LIFT RATIOS AND RELATED PARAMETERS IN THE LEVEL-FLIGHT, CLIMB, AND AUTOROTATIVE-GLIDE CONDITIONS WITH ALTERNATE ROTOR

Test run	V_a (mph)	V (mph)	V_v (ft/min)	γ (deg)	θ_R (deg)	α (deg)	μ	C_L (uncor)	$\Delta\alpha_T$ (deg)	α_{T_a} (deg) (a)	C_L	$\frac{C_L}{\sigma}$	C_T	$\frac{F}{L}$	$\left(\frac{D}{L}\right)_{F_f}$	$\left(\frac{D}{L}\right)_{R_t}$	$\left(\frac{D}{L}\right)_o$	$\left(\frac{D}{L}\right)_T$	$\alpha_{(1.0)(270°)}$ (deg)	$\frac{\left(\frac{D}{L}\right)_{o_R}}{\left(\frac{D}{L}\right)_{o_t}}$
1	46.2	44.8	0	0	-----	-5	0.146	0.421	-6.0	-9.1	0.423	10.12	0.0046	0.254	0.046	0.0023	0	0.206	9.3	0.990
2	46.2	45.4	0	0	-----	-6	.148	.408	-5.8	-9.4	.413	9.84	.0046	.254	.048	.0023	0	.204	9.4	1.010
3	48.3	46.6	0	0	-----	-5	.142	.387	-5.5	-8.8	.391	9.32	.0040	.251	.050	.0022	0	.199	7.8	.962
4	48.3	46.0	0	0	-----	-5	.140	.397	-5.7	-8.8	.402	9.56	.0040	.255	.049	.0022	0	.204	7.8	.972
5	48.3	45.7	0	0	-----	-6	.155	.400	-5.7	-9.0	.405	9.63	.0049	.245	.048	.0024	0	.194	10.5	.979
6	46.8	44.7	0	0	-----	-6	.152	.417	-6.0	-9.1	.422	10.03	.0049	.253	.046	.0024	0	.204	10.4	1.042
7	56.0	54.4	0	0	-----	-7	.177	.282	-4.0	-9.0	.287	6.83	.0046	.234	.068	.0026	0	.163	10.5	1.000
8	55.4	53.8	0	0	-----	-7	.175	.288	-4.1	-9.1	.293	6.97	.0046	.240	.067	.0026	0	.170	10.3	1.043
9	56.9	55.2	0	0	-----	-7	.167	.273	-3.9	-8.9	.278	6.61	.0039	.243	.070	.0025	0	.170	8.5	1.010
10	56.9	55.3	0	0	-----	-7	.167	.273	-3.9	-9.1	.277	6.60	.0039	.239	.071	.0025	0	.166	8.5	.970
11	54.5	54.0	0	0	-----	-8	.183	.305	-4.4	-8.5	.309	7.36	.0052	.238	.063	.0027	0	.172	12.7	1.109
12	54.5	54.0	0	0	-----	-8	.183	.303	-4.3	-8.4	.307	7.31	.0052	.233	.063	.0027	0	.168	12.7	1.058
13	39.0	38.6	0	0	-----	-4	.126	.392	-8.5	-10.7	.398	14.22	.0047	.299	.094	.0021	0	.264	9.1	1.000
14	38.5	38.1	0	0	-----	-4	.124	.604	-8.6	-11.0	.610	14.51	.0047	.300	.033	.0021	0	.265	9.0	.974
15	38.3	38.0	0	0	-----	-4	.116	.612	-8.8	-11.1	.617	14.69	.0042	.331	.033	.0020	0	.296	7.7	1.136
16	38.7	38.4	0	0	-----	-4	.117	.595	-8.5	-10.8	.600	14.29	.0041	.329	.033	.0020	0	.293	7.6	1.123
17	37.0	37.1	0	0	-----	-4	.126	.650	-9.3	-11.4	.656	15.60	.0052	.322	.031	.0021	0	.290	10.4	1.115
18	38.5	38.5	0	0	-----	-4	.131	.600	-8.6	-10.9	.605	14.41	.0052	.302	.033	.0022	0	.267	10.6	1.026
19	64.9	64.9	0	0	10.9	-10	.209	.227	-3.2	-7.8	.231	5.49	.0052	.241	.084	.0033	0	.154	13.8	1.293
20	65.1	65.1	0	0	11.9	-11	.214	.222	-3.2	-8.0	.226	5.38	.0054	.263	.085	.0035	0	.174	14.8	1.573
21	67.2	67.2	0	0	9.2	-10	.203	.210	-3.0	-8.1	.214	5.08	.0045	.237	.091	.0033	0	.142	11.5	1.141
22	74.5	74.5	0	0	10.4	-12	.224	.169	-2.4	-9.6	.174	4.14	.0046	.252	.113	.0041	0	.134	13.0	1.264
23	79.1	79.1	0	0	11.2	-13	.238	.149	-2.1	-10.5	.154	3.67	.0046	.267	.129	.0048	0	.133	14.1	1.334
24	74.2	74.2	0	0	12.4	-13	.236	.168	-2.4	-9.8	.173	4.11	.0050	.280	.114	.0045	0	.162	15.4	1.262
25	38.1	39.4	0	0	8.0	-4	.140	.631	-9.0	-9.9	.638	15.13	.0046	.296	.031	.0020	0	.263	10.8	1.010
26	42.5	43.9	0	0	9.4	-5	.163	.508	-7.2	-9.0	.507	12.07	.0053	.266	.038	.0022	0	.226	10.9	.990
27	69.6	70.9	0	0	12.4	-10	.229	.186	-2.7	-9.1	.190	4.53	.0051	.266	.109	.0041	0	.179	15.2	1.845
28	45.1	45.9	0	0	10.0	-6	.157	.441	-6.3	-8.1	.445	10.59	.0055	.253	.044	.0023	0	.207	12.3	1.044
29	42.5	43.4	0	0	11.4	-6	.150	.494	-7.1	-8.5	.498	11.85	.0056	.312	.039	.0023	0	.262	13.9	1.450
30	82.2	82.2	0	0	10.9	-24	.241	.131	-1.9	-11.3	.137	3.25	.0042	.290	.147	.0052	0	.138	13.2	1.425
31	80.0	80.0	0	0	11.0	-14	.240	.135	-1.9	-11.3	.141	3.35	.0043	.283	.143	.0051	0	.135	13.4	1.389
32	78.4	80.4	0	0	10.6	-13	.236	.140	-2.0	-10.9	.146	3.48	.0043	.279	.137	.0048	0	.131	13.1	1.306
33	79.8	80.8	0	0	10.9	-13	.237	.137	-2.0	-11.2	.142	3.39	.0042	.284	.141	.0049	0	.138	13.1	1.430
34	32.3	32.1	753	13.5	10.8	-22	.098	.838	-12.0	-29.2	.858	20.27	.0050	.685	.030	.0018	.277	.376	9.7	1.058
35	34.1	33.8	790	13.4	-----	-22	.103	.749	-10.7	-28.1	.763	18.15	.0049	.654	.033	.0019	.276	.344	9.8	1.040
36	45.2	46.2	807	11.4	-----	-20	.142	.400	-5.7	-20.6	.410	9.75	.0049	.480	.051	.0028	.202	.224	11.2	1.161
37	33.0	32.8	771	13.5	9.6	-20	.095	.816	-11.7	-28.6	.830	19.79	.0044	.669	.030	.0018	.277	.360	7.3	.938
38	28.0	27.9	607	14.3	10.7	-19	.086	1.148	-16.4	-32.0	1.157	27.55	.0050	.742	.028	.0018	.255	.462	9.3	.994
39	45.5	47.3	304	4.2	12.9	-13	.157	.444	-6.4	-18.2	.451	10.73	.0059	.393	.044	.0024	.073	.274	14.1	1.677
40	49.8	51.0	505	6.4	12.4	-15	.165	.364	-5.2	-14.4	.372	8.86	.0055	.386	.055	.0025	.113	.215	13.5	1.858
41	63.1	62.0	-1838	-23.1	-----	4	.201	.221	-3.2	5.4	.221	5.25	.0045	-.013	.080	.0030	-.255	.137	----------	1.078
42	52.5	51.0	-1053	-13.6	-----	8	.166	.318	-4.6	6.8	.317	7.55	.0045	-.017	.056	.0024	-.242	.167	----------	1.011
43	53.1	54.6	-1065	-12.8	4.8	7	.179	.305	-4.4	6.2	.304	7.23	.0050	-.015	.056	.0025	-.228	.158	----------	.986
44	49.2	50.3	-1100	-14.4	5.6	8	.168	.362	-5.2	7.2	.361	8.59	.0053	-.016	.049	.0025	-.256	.189	----------	1.164
45	43.0	44.7	-1022	-15.1	5.6	10	.148	.460	-6.6	7.2	.458	10.91	.0052	-.015	.039	.0022	-.269	.213	----------	1.042

[a] α_{T_a} = Shaft inclination (obtained from table II) + $\Delta\alpha_T$.

NACA

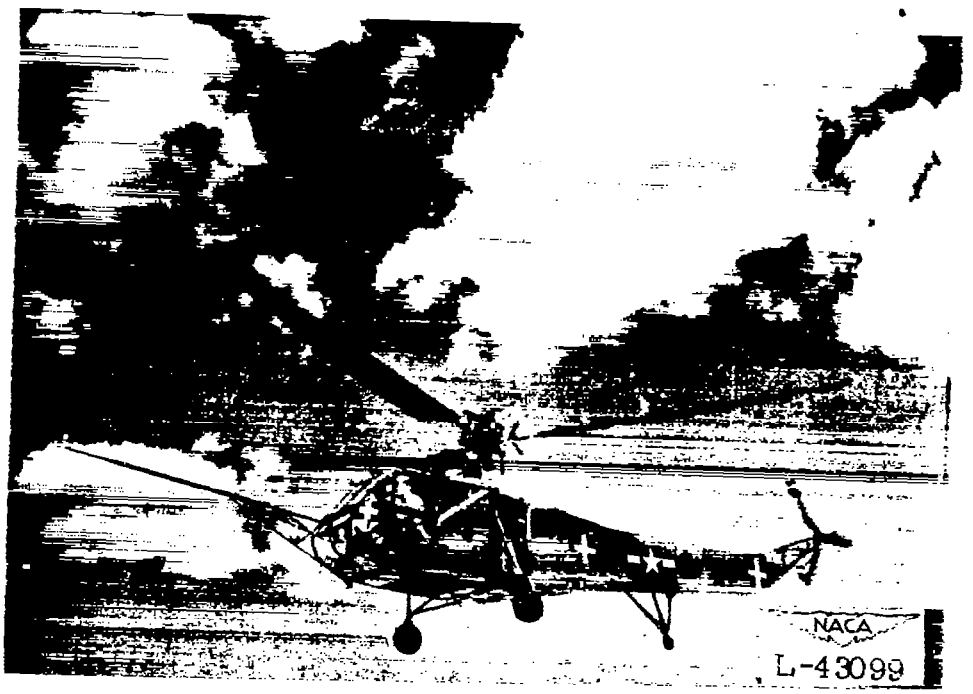

Figure 1.- General view of test helicopter equipped with the original-production rotor.

Main rotor:	
Radius, ft	19
Disk area, sq ft	1134.1
Ratio of rotational speed to engine speed	0.107
Tail rotor:	
Radius, ft	3.96
Blade area (3 blades), sq ft	4.92
Disk area, sq ft	49.2
Ratio of rotational speed to engine speed	0.567
Center line of main rotor to center line of tail rotor, ft	25.19
Parasite-drag area, sq ft	22.92
Rated horsepower	180

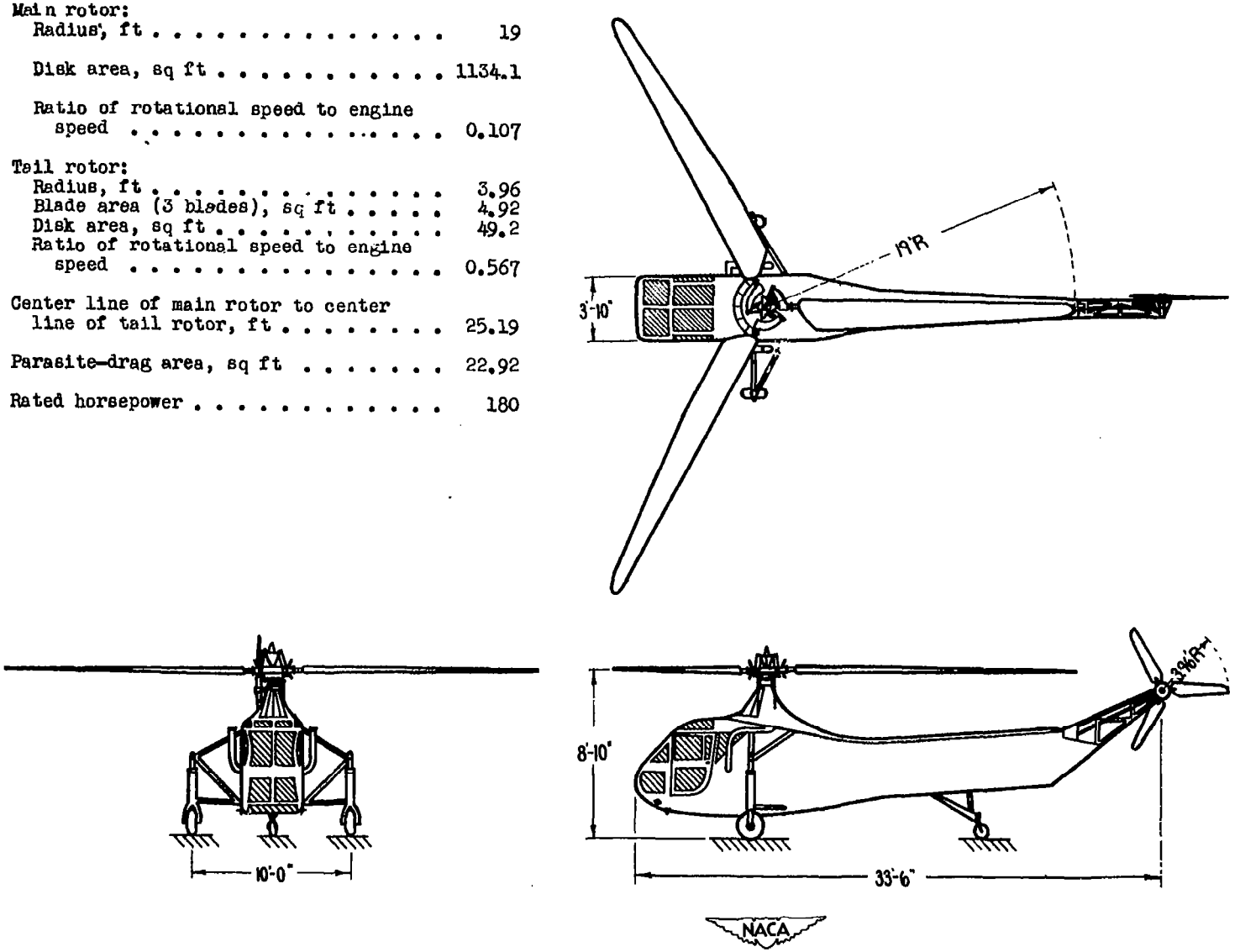

Figure 2.- Dimensions and characteristics of test helicopter. (All dimensions are in inches.)

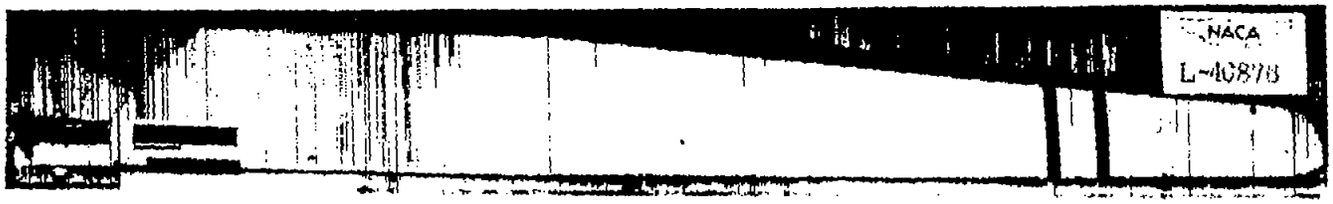

Original blade

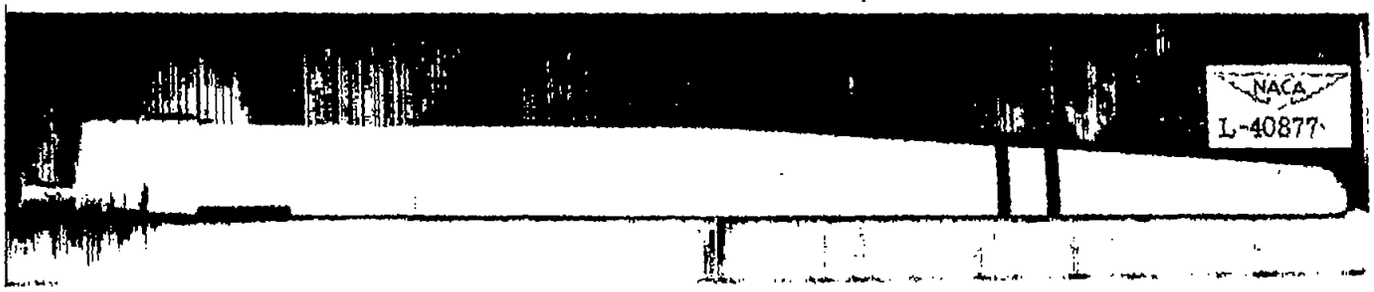

Alternate blade

(a) General views.

Figure 3.- General views illustrating surface condition and sketches giving plan-form dimensions of original and alternate main-rotor blades.

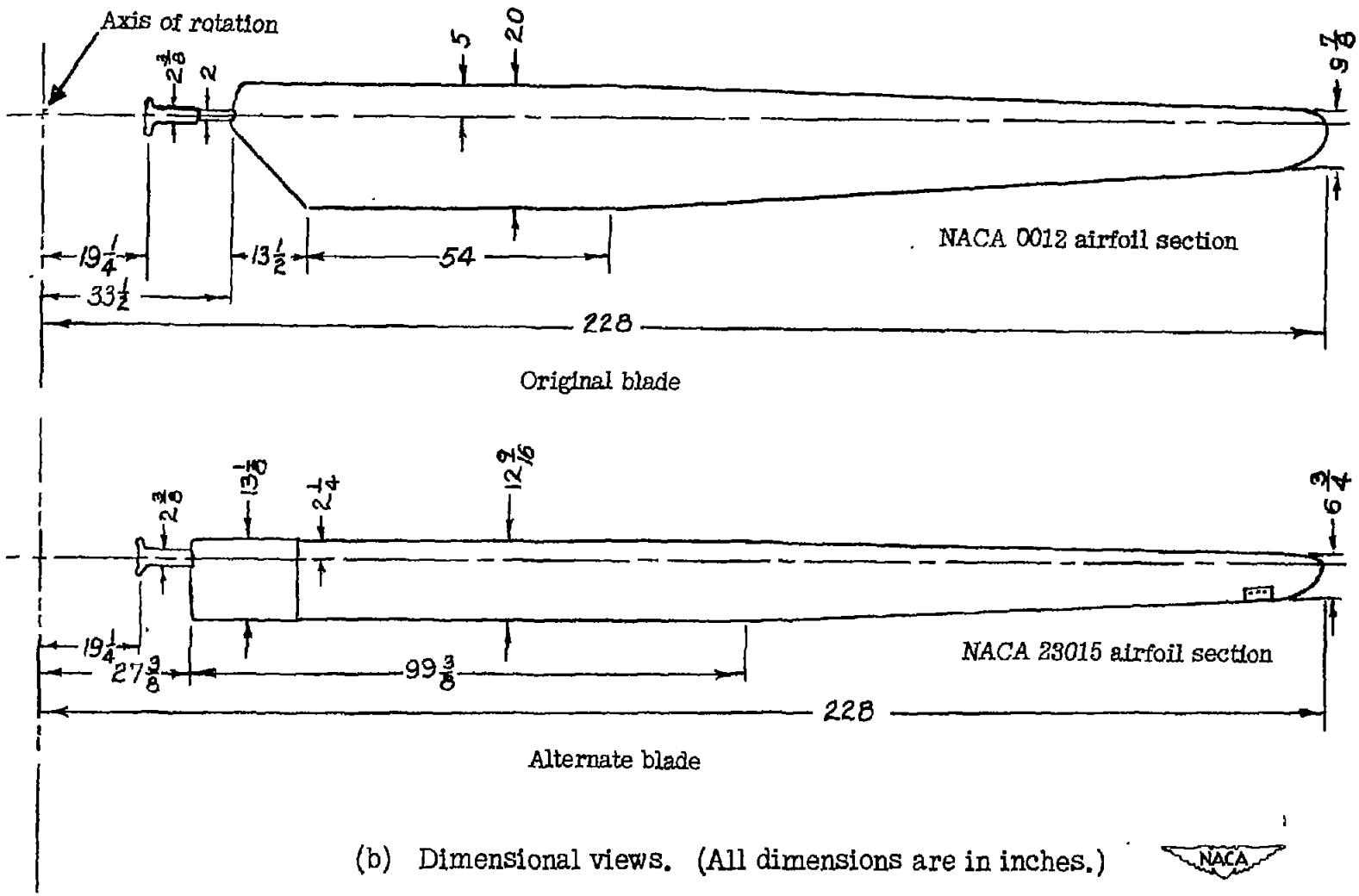

(b) Dimensional views. (All dimensions are in inches.)

Figure 3.- Concluded.

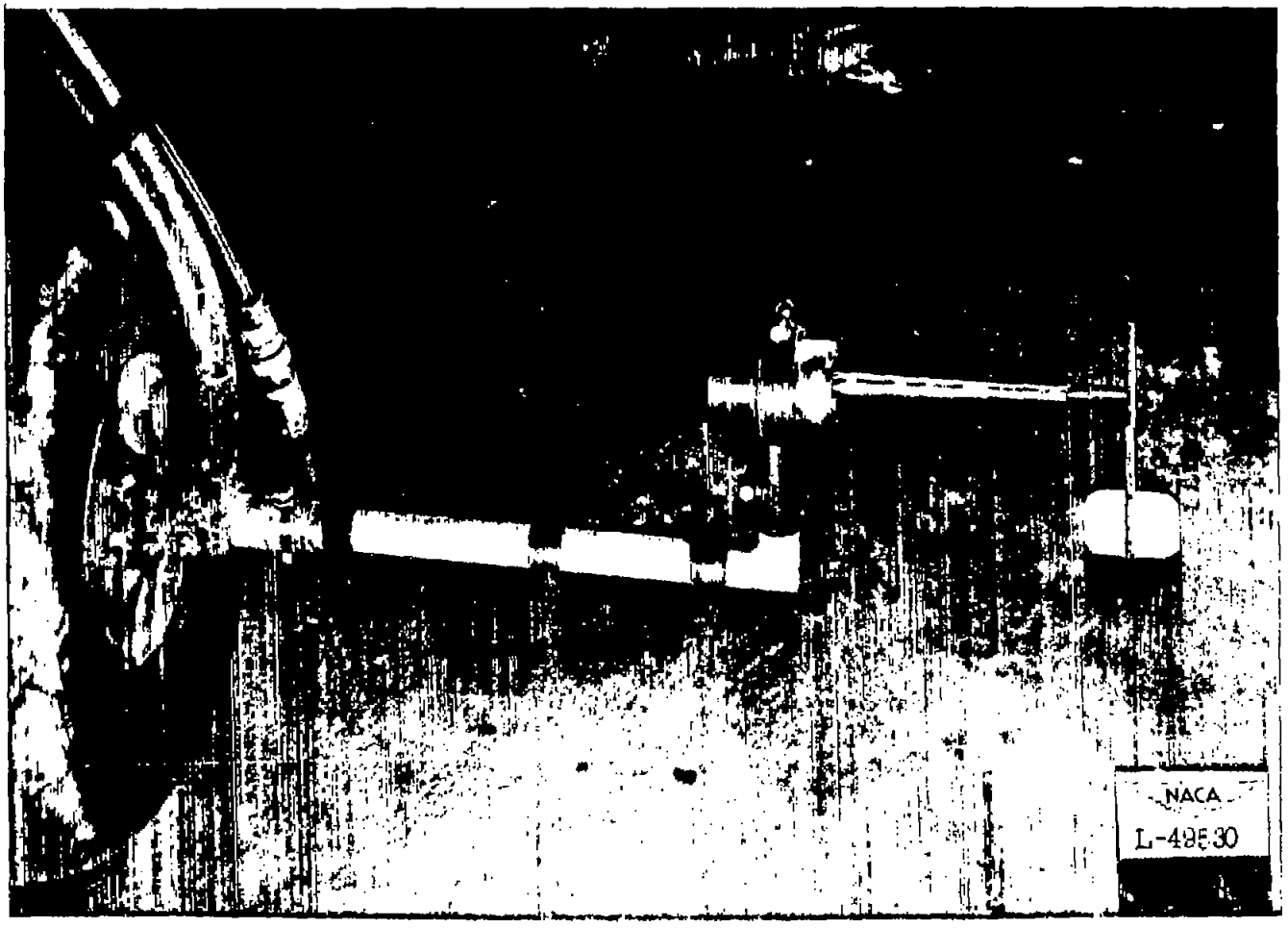

Figure 4.- Yaw vane and transmitter used to indicate and record deviations from zero longitudinal airspeed in vertical descent.

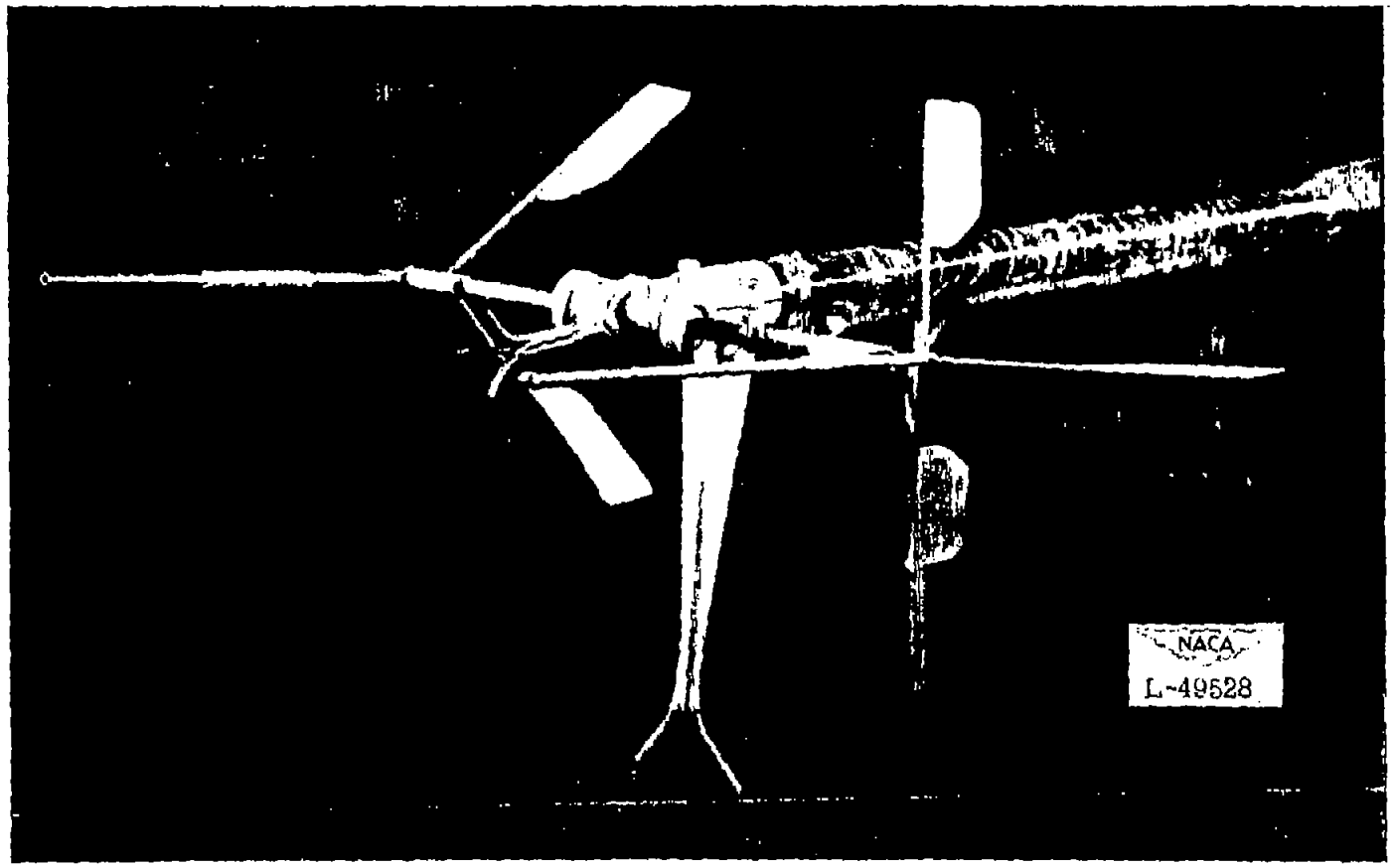

Figure 5.- Detail of airspeed head, showing vertical yaw fork used to record deviation from zero lateral airspeed in vertical descent.

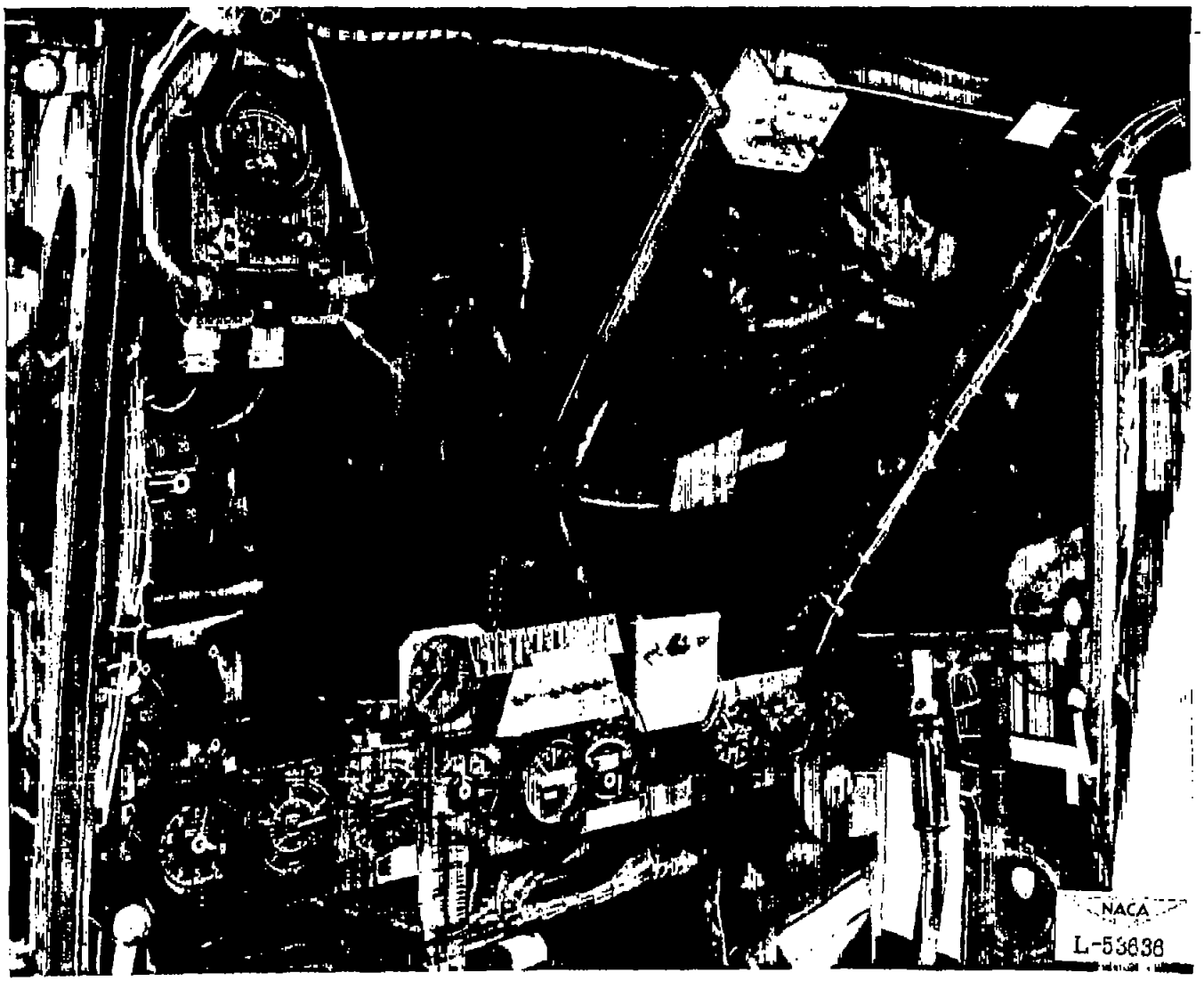

Figure 6.- General view of cockpit indicating instruments. (Arrow shows pith-ball indicator.)

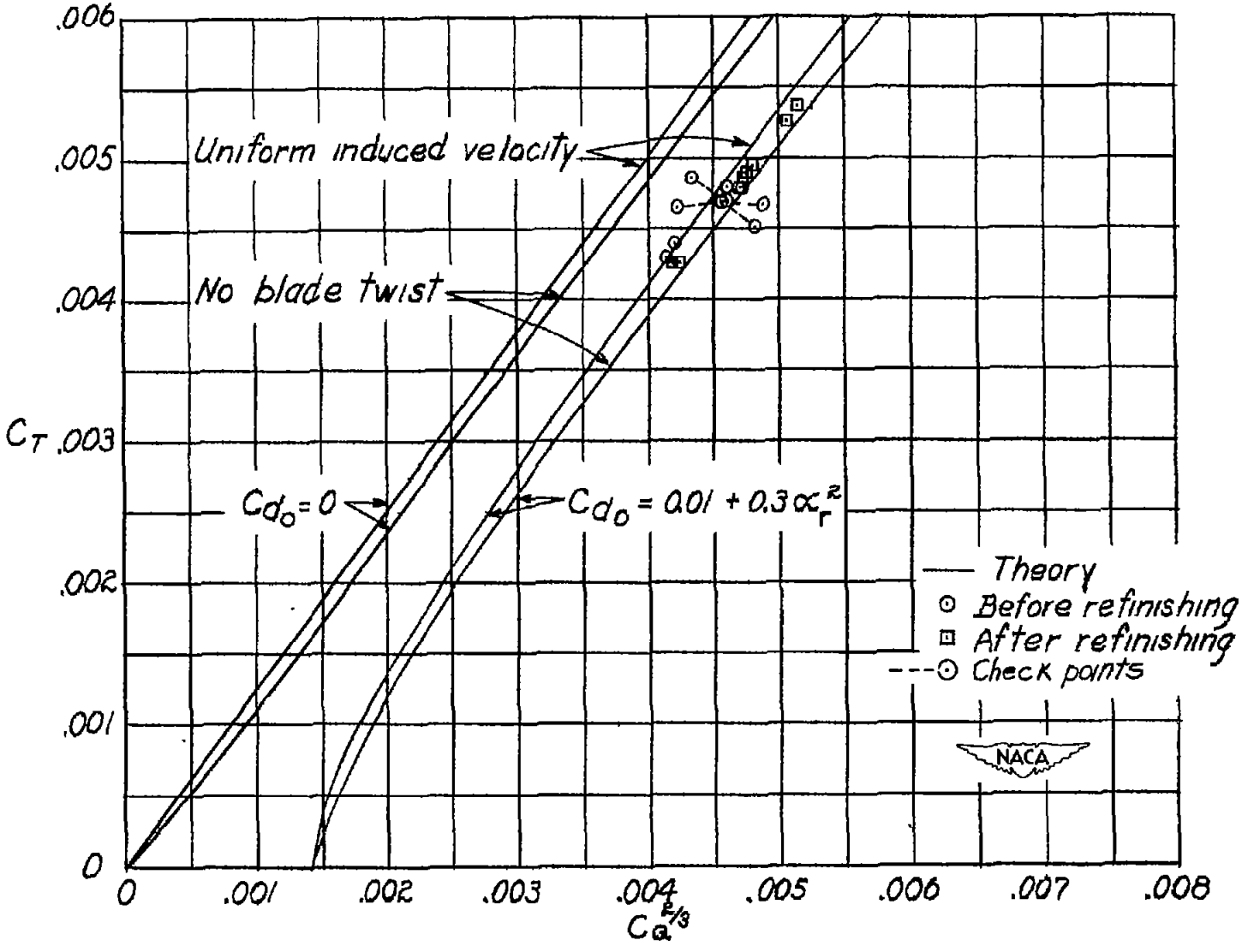

Figure 7.- Comparison of experimental hovering performance of alternate rotor with theory.

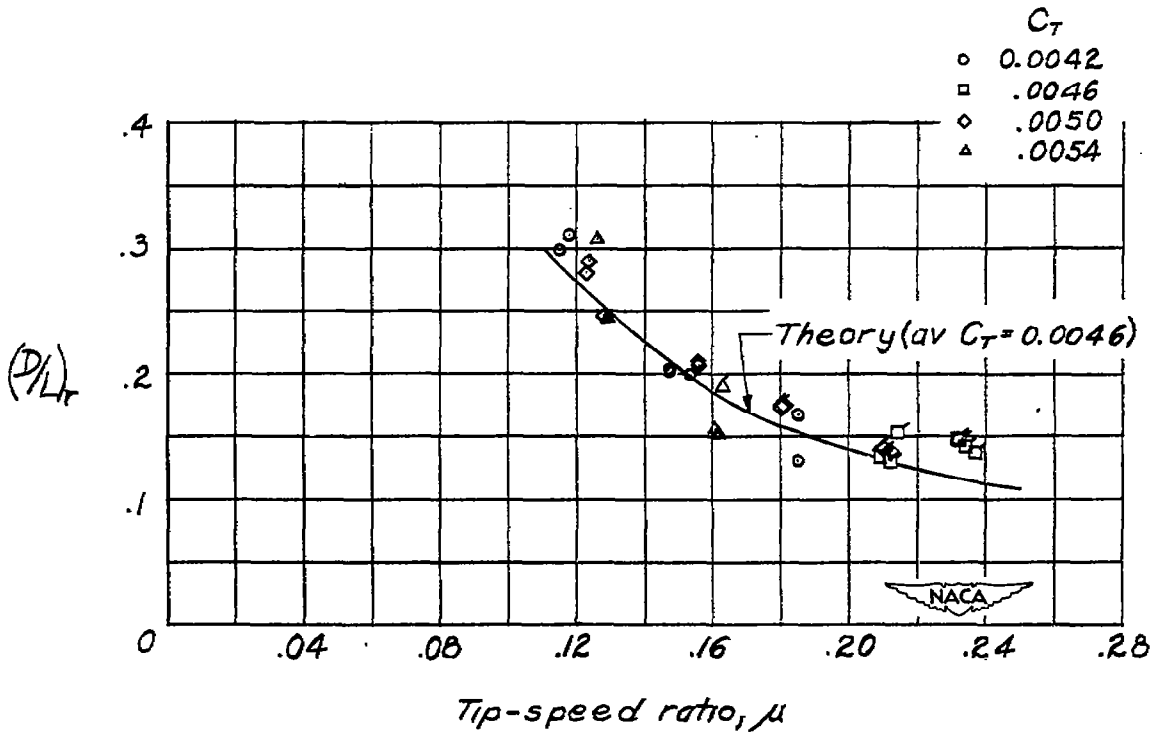

(a) Before refinishing.

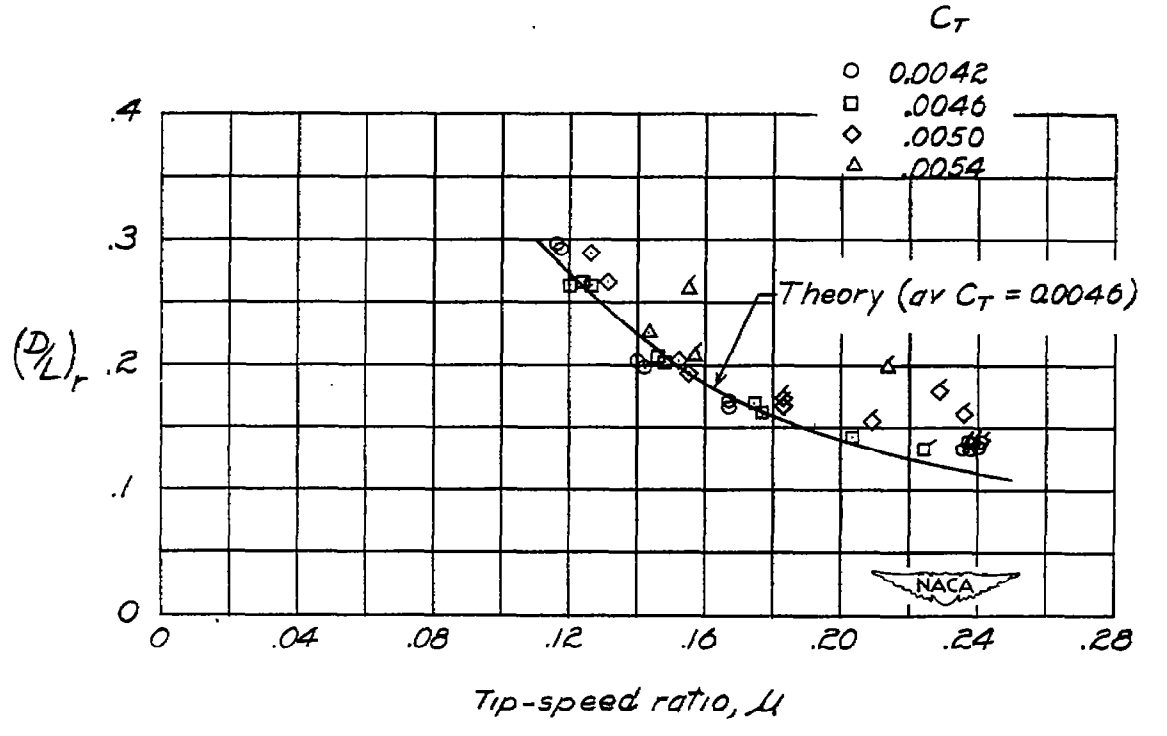

(b) After refinishing.

Figure 8.- Comparison of level-flight performance of alternate rotor with theory. (Flagged points represent conditions for which the calculated tip angle of attack of the retreating blade is greater than 12°.)

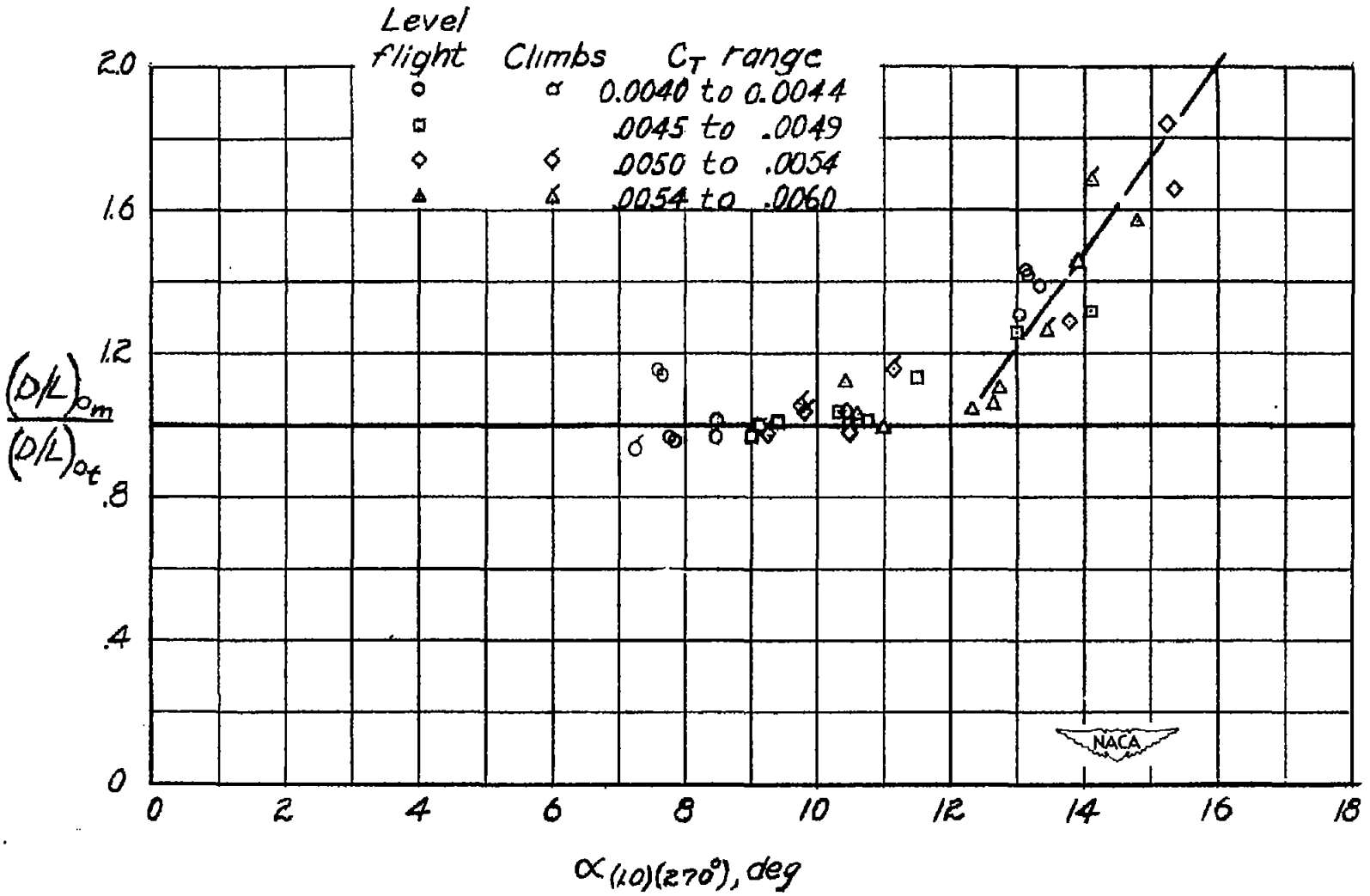

Figure 9.- Effect of blade stalling on the comparison between measured and calculated performance in level flight and in climb for the alternate rotor.

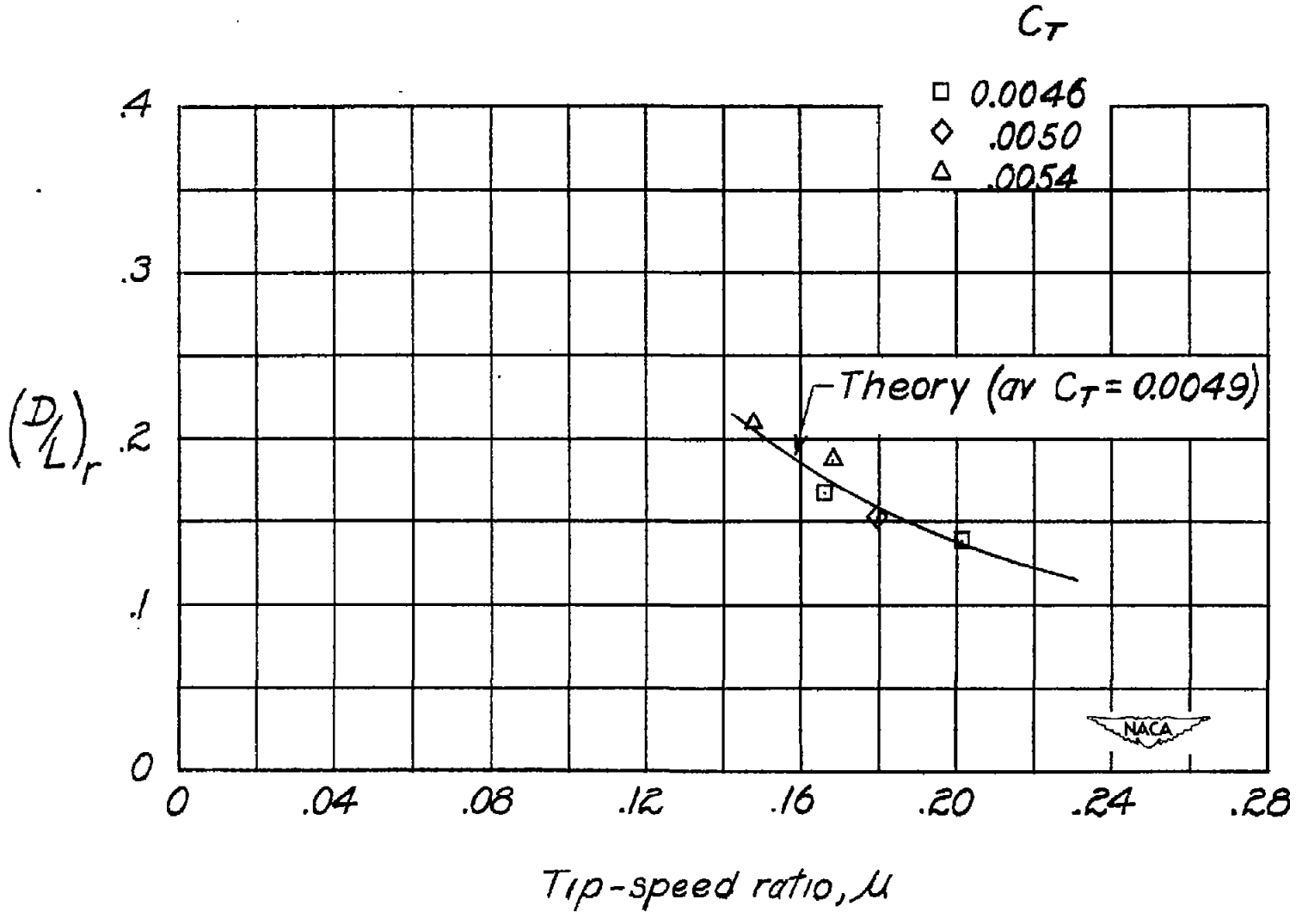

Figure 10.- Comparison of experimental autorotative-glide performance of alternate rotor with theory.

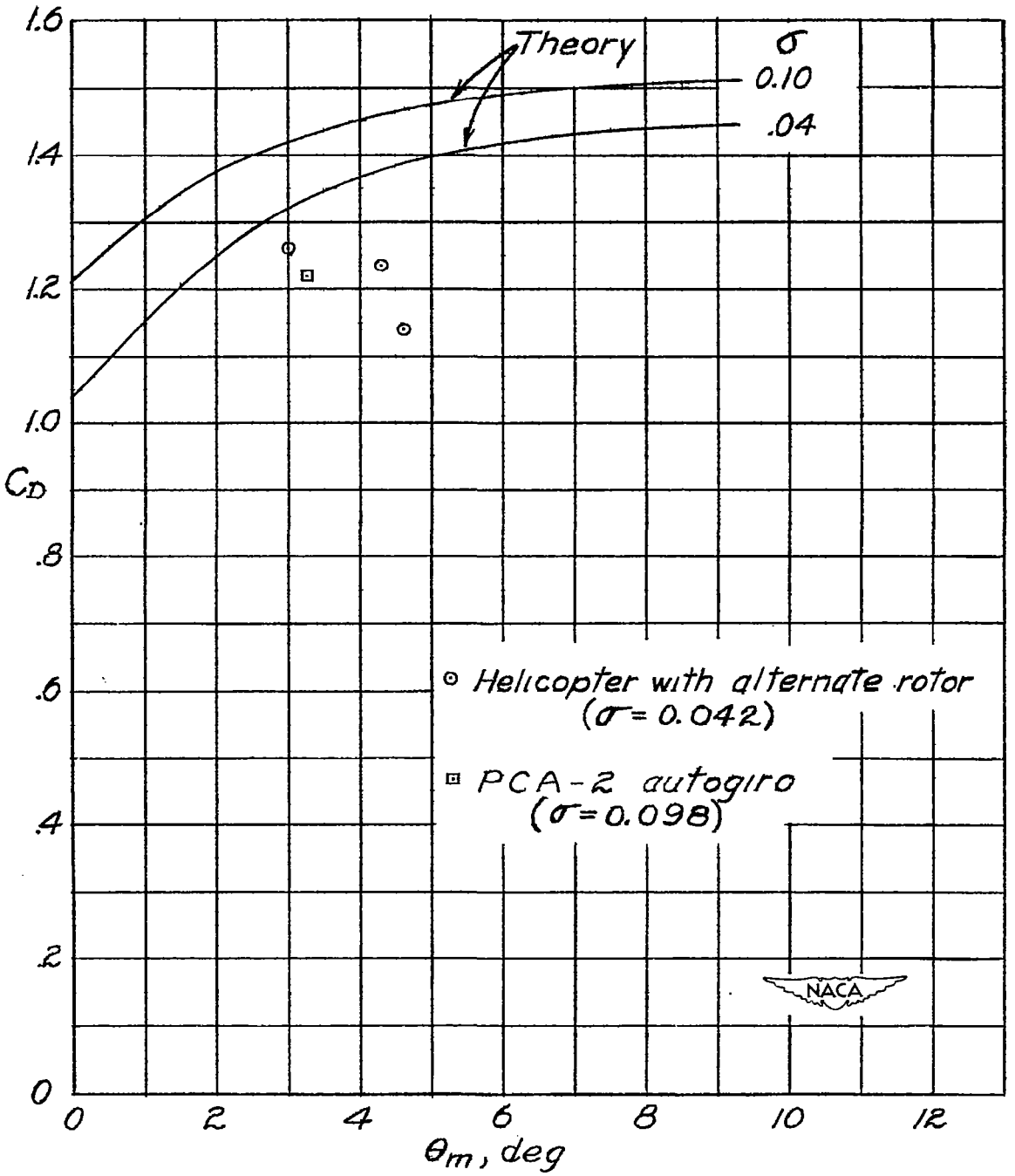

Figure 11.- Comparison of vertical autorotative performance of alternate rotor with the semiempirical theory for untwisted blades.

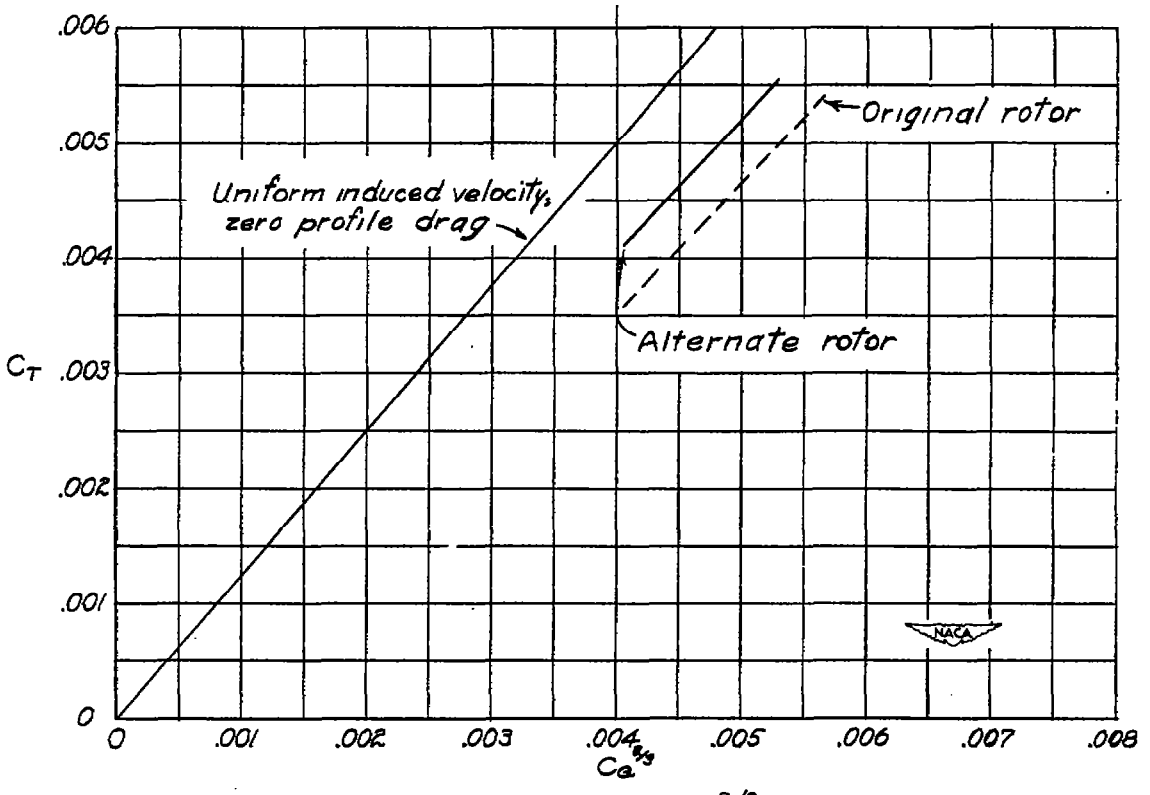

(a) C_T against $C_Q^{2/3}$.

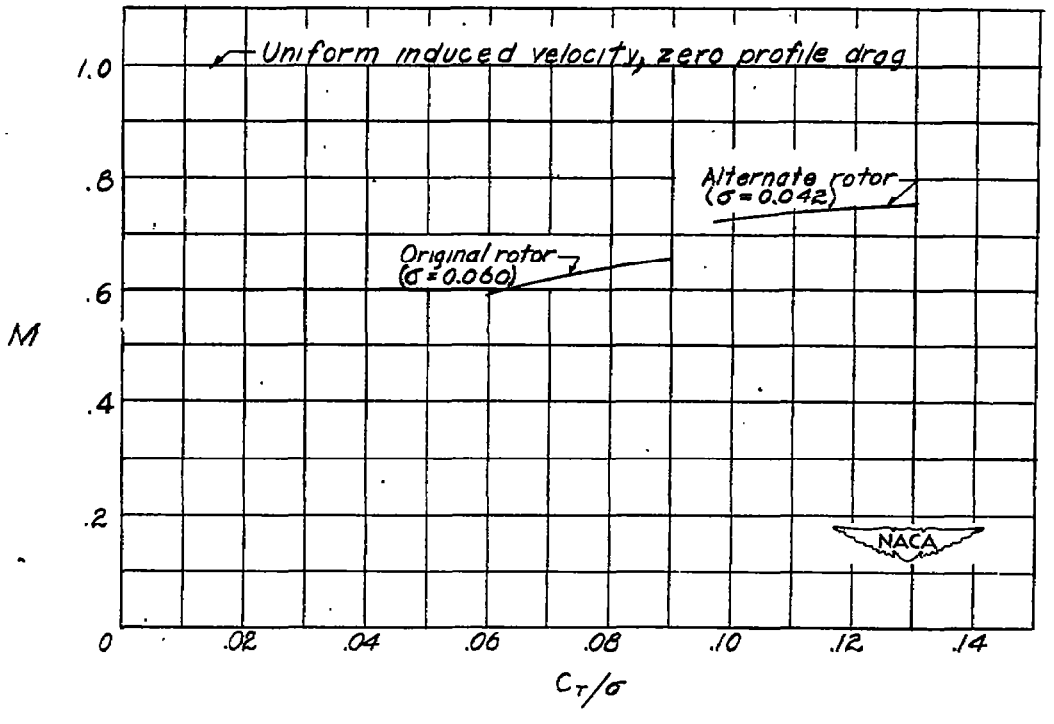

(b) Rotor figure of merit M against C_T/σ.

Figure 12.- Comparison of hovering performance of original-production rotor and the alternate test rotor.

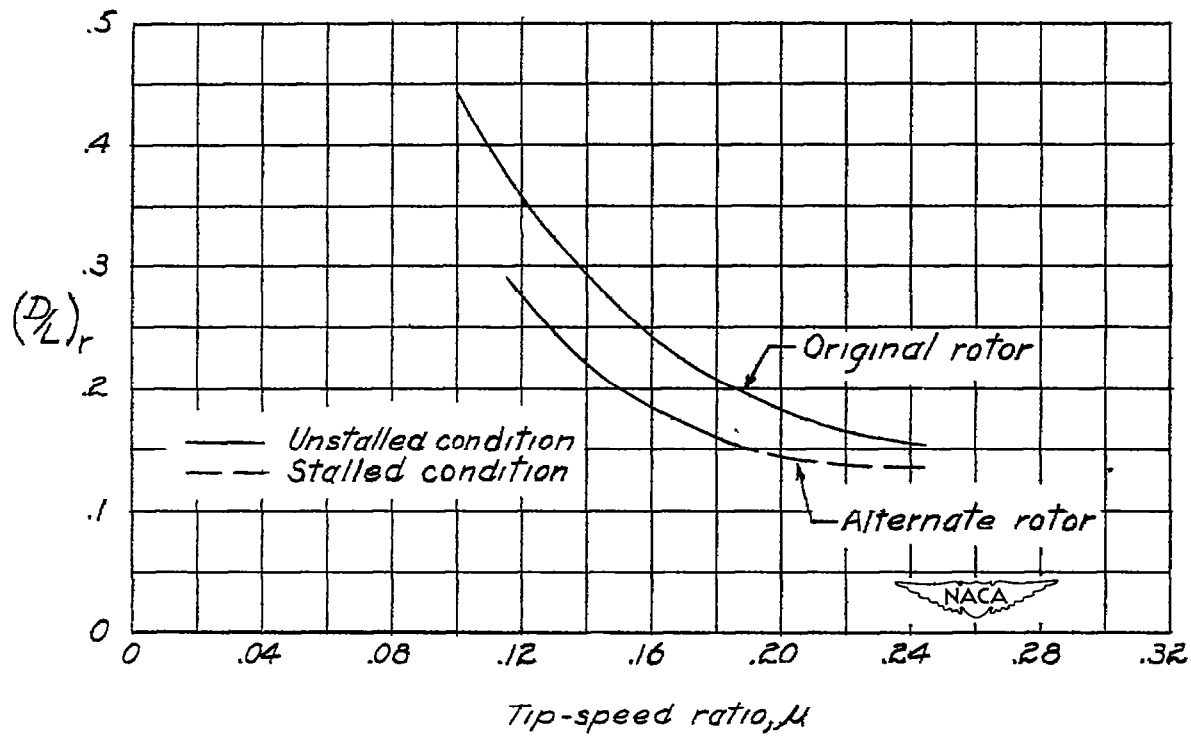

(a) General rotor performance.

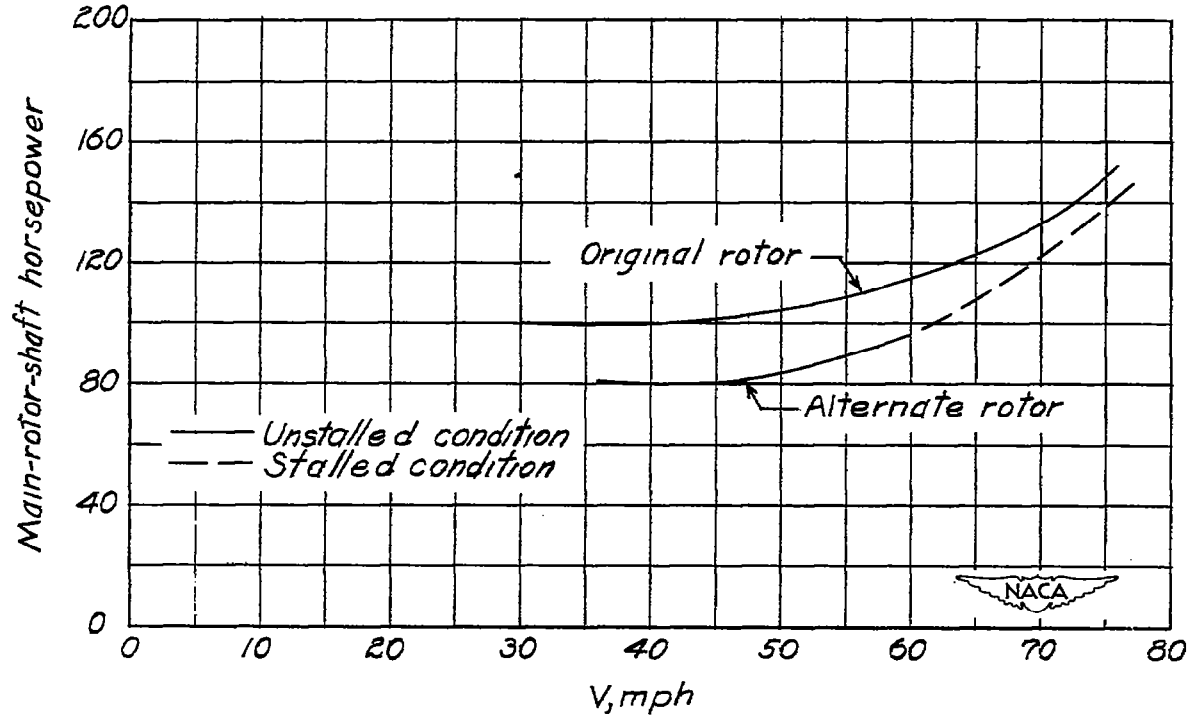

(b) Sea-level performance, W = 2565 pounds.

Figure 13.- Comparison of level-flight performance of test helicopter with the original-production rotor and with the alternate rotor. Average C_T = 0.0046.

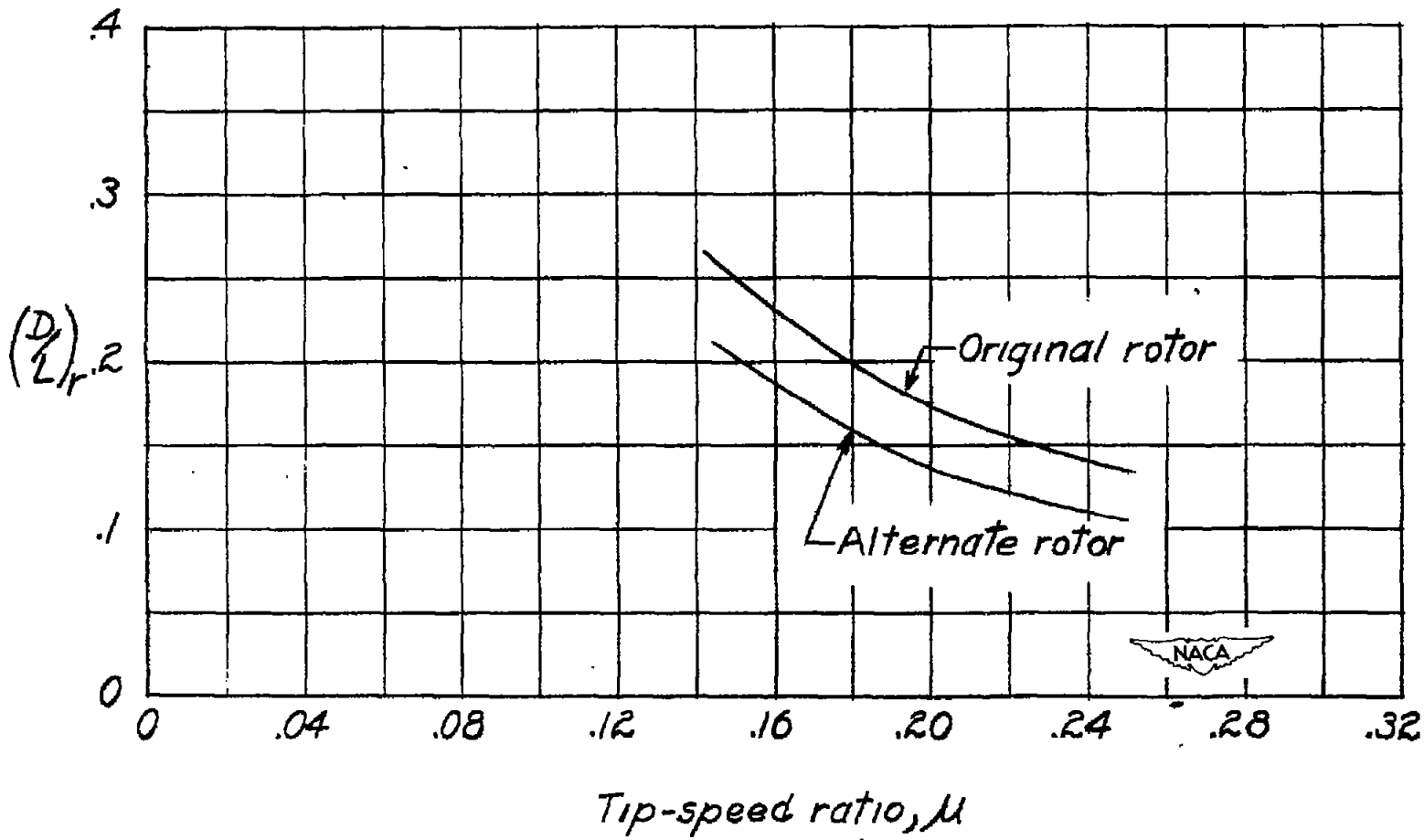

Figure 14.- Comparison of the autorotative-glide performance of the original-production rotor and the alternate test rotor. Average C_T = 0.0049.